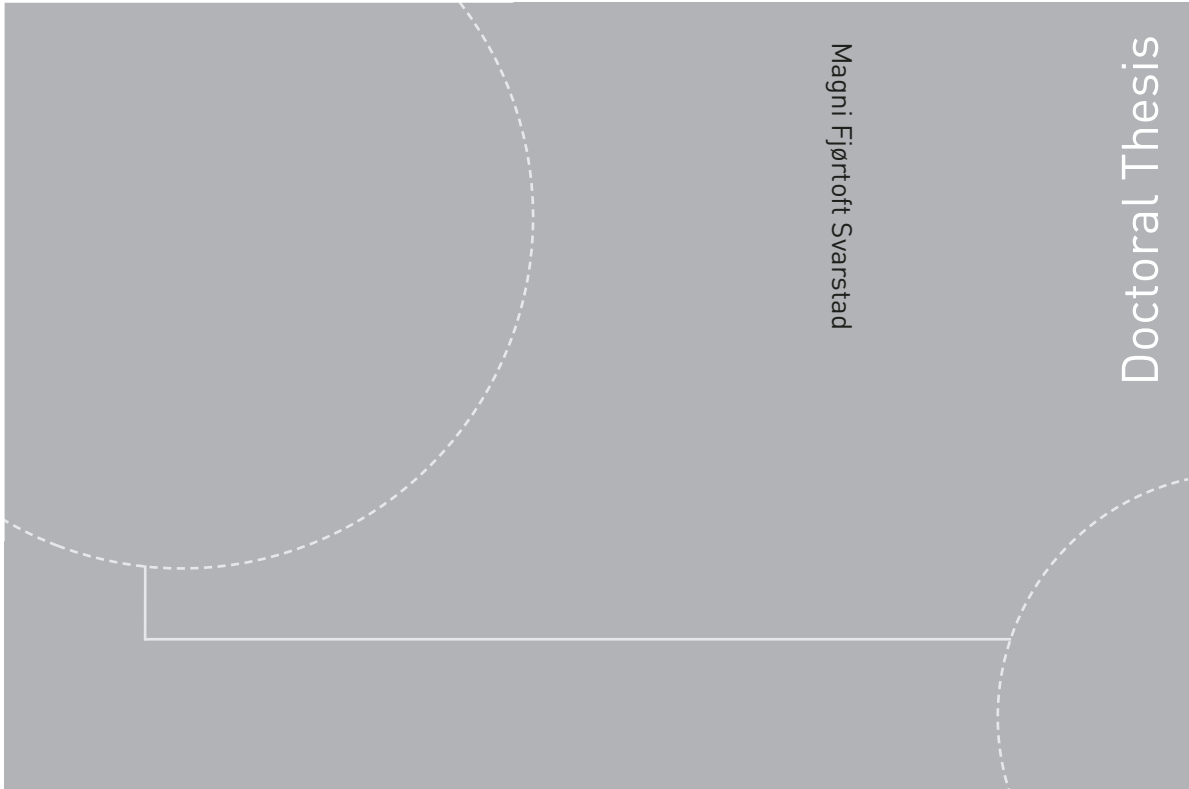


Doctoral theses at NTNU, 2019:49

Magni Fjørtoft Svarstad

# Fast Transition between Operational Modes of a Reversible Pump-Turbine



ISBN 978-82-326-3702-7 (printed version)  
ISBN 978-82-326-3703-4 (electronic version)  
ISSN 1503-8181

Doctoral theses at NTNU, 2019:49

**NTNU**  
Norwegian University of  
Science and Technology  
Faculty of Engineering  
Department of Energy and Process Engineering

Magni Fjørtoft Svarstad

# Fast Transition between Operational Modes of a Reversible Pump-Turbine

Thesis for the degree of Philosophiae Doctor

Trondheim, February 2019

Norwegian University of Science and Technology  
Faculty of Engineering  
Department of Energy and Process Engineering



Norwegian University of  
Science and Technology

**NTNU**

Norwegian University of Science and Technology

Thesis for the degree of Philosophiae Doctor

Faculty of Engineering

Department of Energy and Process Engineering

© Magni Fjørtoft Svarstad

ISBN 978-82-326-3702-7 (printed version)

ISBN 978-82-326-3703-4 (electronic version)

ISSN 1503-8181

Doctoral theses at NTNU, 2019:49



Printed by Skipnes Kommunikasjon as

Men sammen så veie vi fleire tonn  
Med littegrann hjelp gjer det  
littegrann monn  
Det e itjnå som kjem tå sæ sjøl

---

*Vømmøl spellemannslag*

*Til Anna og Vilde - det beste i livet*



# Abstract

The future demands of energy production to balance more intermittent energy sources creates two main technical challenges for the hydro power production. Increased off-design operation, including both operation outside Best Efficiency Point and more starts and stops, are needed to facilitate use of more intermittent energy resources. In addition to this there is a demand for rapid change between storing and generating energy in pump storage power plants.

There is therefore a need to improve the fundamental understanding of transient operation of the reversible pump turbine during different modes of operation. The present work investigates the four quadrant characteristics of a reversible pump-turbine. With focus on the fast transition between pump and turbine mode of operation. The research has consisted of both experimental work and transient simulation.

A fast transition is described in this thesis as a method to change from pump to turbine mode of operation, using the head to change the direction of the pump-turbines rotational speed from pump to turbine direction. The procedure start in normal pump mode of operation and end at idle speed in turbine mode of operation, and the guide vanes are open during the whole transition.

The most important contributions in this thesis is connected to the fast transition, where the field experiments is a proof of concept for the fast transition method. The pressure pulsations during the fast transition are also compared to a normal procedure of change from pump to turbine mode of operation. The fast transition is also simulated using a 1D numerical model capable of simulating both pump and turbine mode of operation. The laboratory characteristics have been important in comparison to the improved 1D simulation model. The numerical and measured results show a good correlation.



# Acknowledgements

The Waterpower laboratory at NTNU has now been a part of my life for six years. First as a master student, then as a scientific assistant and finally as a PhD-student. The environment created in the lab, with its collaborative atmosphere and camaraderie, give room for open, candid professional discussions. All the people contributing to the special atmosphere in the lab are a big part of my decision to become a PhD-student.

My gratitude to my supervisor Torbjørn Nielsen, and co-supervisors Ole Gunnar Dahlhaug and Pål-Tore Storli, for all the guidance, discussions and suggestions throughout my work. A special thanks to my colleagues in the lab for help, discussions, encouragements and making these years filled with funny projects and silly discussions.

For letting me do measurements a bit outside of the normal operation, and helping me achieve them, thank you to Odd Karsten Pettersen, Lars Magnus Brækken and Oddvar Lundseng at NTE, and Ragnar Eide at Hymatek.

Through these years a number of people have at some point given me guidance and supported this project, I thank you all.

Last, but not least. Thank you so much to Jo Røed Skårderud. Who have not only held the family together, but showed a remarkable patience with me during the ups and downs of this work. Thank you for helping me present my work in an understandable manner to people outside the world of hydro power. Thank you for lifting me up, encouraging me and being in my life. This work would never have been completed without you and I love you for this, and a thousand things more!



# Contents

<b>List of Tables</b>	<b>xi</b>
<b>List of Figures</b>	<b>xiii</b>
<b>List of Symbols</b>	<b>xv</b>
<b>I Thesis</b>	<b>1</b>
<b>1 Introduction</b>	<b>3</b>
1.1 Research overview . . . . .	3
1.2 Motivation . . . . .	3
1.3 Objective . . . . .	5
1.4 Contributions . . . . .	5
<b>2 Theoretical background</b>	<b>7</b>
2.1 Introduction to reversible pump-turbines . . . . .	7
2.2 Characteristics of reversible pump-turbine . . . . .	9
2.2.1 Off-design conditions . . . . .	11
2.2.2 System influence on characteristics . . . . .	12

2.3	One dimensional transient simulation . . . . .	13
<b>3</b>	<b>Research methods</b>	<b>17</b>
3.1	Laboratory measurements . . . . .	17
3.1.1	Transient flow rate measurement . . . . .	18
3.1.2	Experimental procedure . . . . .	19
3.2	Prototype measurements . . . . .	19
3.2.1	Normal procedure . . . . .	20
3.2.2	Fast transition . . . . .	21
3.2.3	Rainflow counting method . . . . .	21
3.3	Transient simulation . . . . .	22
<b>4</b>	<b>Summary of papers</b>	<b>25</b>
<b>5</b>	<b>General discussion</b>	<b>27</b>
5.1	Prototype measurements . . . . .	28
5.2	Simulation model . . . . .	30
<b>6</b>	<b>Conclusion</b>	<b>33</b>
<b>7</b>	<b>Further work</b>	<b>35</b>
<b>II</b>	<b>Papers</b>	<b>41</b>
	<b>Paper 1</b>	
	<i>Fast Transition from Pump to Turbine mode of Operation</i>	
	Svarstad, M. F., Nielsen, T. K.	
	<i>International Journal of Fluid Machinery and Systems</i>	
	vol. 11, 2018	<b>43</b>
	<b>Paper 2</b>	

*Pressure pulsations during a fast transition from pump to turbine mode of operation in laboratory and field experiment*

Svarstad, M. F., Nielsen, T. K.

*IOP Conference series*

2018

53

**Paper 3**

*A comparison of pressure pulsations during normal and fast transition from pump to turbine mode of operation*

Svarstad, M. F., Nielsen, T. K.

*Submitted*

2018

67

**Paper 4**

*Four quadrant characteristics simulated with 1D RPT model*

Svarstad, M. F., Nielsen, T. K., Storli P. T.

*Submitted*

2018

79



# List of Tables

2.1	Simulation parameters . . . . .	15
3.1	Model RPT parameters . . . . .	18
3.2	Key parameters Tevla . . . . .	20



# List of Figures

2.1	Pump-turbine power plant . . . . .	8
2.2	Ranges of runner geometries . . . . .	8
2.3	Four quadrant characteristics . . . . .	9
2.4	Velocity diagram . . . . .	11
3.1	Laboratory test loop . . . . .	18
3.2	Field instrument position . . . . .	20
3.3	Rainflow counting method . . . . .	22
5.1	Pressure amplitudes during FT and NP . . . . .	28
5.2	Simulation of FT . . . . .	30
5.3	HQ characteristics . . . . .	31



# List of Symbols

## Latin Symbols

$A$	Area	$m^2$
$A_{eq}$	Equivalent area, air cushion chamber	$m^2$
$B$	Inlet height runner	$m$
$C$	Absolute velocity component	$m/s$
$D$	Diameter	$m$
$g$	Gravitational acceleration	$m/s^2$
$H$	Head	$m$
$h$	reduced head	—
$k$	Friction factor	
$L$	Length	$m$
$m_s$	Reduced starting torque	—
$n$	Rotational speed	$rev/s$
$n_{ED}$	Speed factor	—
$N_{QE}$	Specific speed	—
$p$	Pressure	$kPa$
$Q$	Flow rate	$m^3/s$

$q$	Reduced flow rate	—
$Q_{ED}$	Discharge factor	—
$r$	Radius	$m$
$R_q$	Geometrical parameter	$1/m$
$r_q$	Reduced $R_q$	—
$t$	Time	$s$
$T_a$	Time constant, rotating inertia	—
$T_w$	Time constant, hydraulic inertia	—
$U$	Circumferential velocity component	$m/s$
$W$	Relative velocity component	$m/s$

**Greek Symbols**

$\alpha$	Guide vane opening angle	$^\circ$
$\alpha_{idle}$	$\alpha$ to achieve idle speed	
$\beta$	Angle between $U$ and $W$	
$\eta$	Efficiency	—
$\kappa$	Opening degree	—
$\omega$	Rotational speed	$1/s$
$\psi$	Reduced geometric parameter	—
$\rho$	Density	$kg/m^3$
$\sigma$	Parameter with $\eta$ and $\psi$	—
$\tilde{\omega}$	Reduced $\omega$	—
$\tilde{T}_m$	Reduced generator torque	—
$\zeta$	Friction loss	$kPa$

**Abbreviation**

$1D$	One dimensional
------	-----------------

<i>BEP</i>	Best Efficiency Point
<i>CFD</i>	Computational Fluid Dynamics
<i>EMF</i>	Electromagnetic Flow Meter
<i>FT</i>	Fast Transition
<i>GV</i>	Guide vanes, wicket gate
<i>PSPP</i>	Pumped Storage Power Plant
<i>RPT</i>	Reversible Pump-Turbine

**Indices**

*	Rated value, equal index $r$
1	Position indication, inlet runner from turbine perspective
2	Position indication, outlet runner from turbine perspective
$e$	End of time period
$i$	Step in time period
$pt$	Pressure tank
$r$	Rated value
$s$	Start of time period



**Part I**

**Thesis**



# Chapter 1

## Introduction

---

■ The chapter introduces the work presented in this thesis. Focusing on motivation, objectives and research contributions of the work.

---

### 1.1 Research overview

The research in this thesis consists of three methods of investigation: laboratory measurements, field measurements and numerical simulations. All methods are concentrated on the transient behavior of a reversible pump-turbine, in a manner described in the objectives presented below. The results of the research are presented in four papers found in full format in Part II of this thesis, the research contribution in each paper is presented in Section 1.4. The three methods of investigation are further described in Chapter 3 and a summary of the papers can be found in Chapter 4.

### 1.2 Motivation

With the human made climate change, the world need to change the way we produce energy [1]. Norway's hydro power production is not only affected by, but can be a positive contribution in those changes. To highlight the mechanisms behind the change in hydro power production we need to first remember Norwegian hydro powers modern beginning. In Norway's history, hydro power was the foundation for the industrialization of the country. The aluminum, and other, energy intensive industries needed a high amount of cheap power, and with its high mountains and

abundant rain Norway could supply the needed energy through hydro power. The result was that the first large scale hydro power plants was built with the industry in mind [2]. What followed, somewhat simplified, was a situation where almost all the energy needs of Norway's industry and inhabitants was delivered by hydro power.

A common claim is that the liberalization of the energy market resulted in more off-design operation and an increase in start and stop cycles. For the Norwegian energy market, this claim is a simplification. 48 % of the units had an increase in the start and stop cycles, while the average for all units is approximately constant [3]. The same trend is seen with off-design operation, where some power plants have more operation outside best efficiency point (BEP), while in other units the off-design operation is reduced.

Both the final results from climate change and the worlds willingness to change towards a low-carbon society are uncertain. Even among those who agree that a shift in energy production is necessary, there is a number of possible routs and hurdles along the way.

With many uncertainties, some areas are clear. *Renewables Global Status Report (REN21)* points at the need to balance the energy production from intermittent renewable energy resources. Both to utilize the surplus energy when energy production is higher than the demand, and to store energy for times when the production is to low [4]. Hydro power, in addition to being a renewable resource itself, can and are being used to enable energy production from other renewable energy sources. Regarding energy storage, pumped storage power plants (PSPP) are already the most common way to store energy with a global installed capacity of 153 GW [4].

The ramifications of climate change already upon us, and the future of the energy production, creates two main technical challenges for the hydro power production of tomorrow:

**First:** Increased off-design operation, including both operation outside BEP and more starts and stops, are needed to facilitate use of more intermittent energy resources.

**Second:** Increased demand for rapid change between storing and generating energy in PSPP.

## 1.3 Objective

**The fast transition (FT)** is in this work defined as the method to change between storing and generating mode of operation using the head to change the direction of the machines rotational speed from pump to turbine direction, and without the need to close the guide vanes during the transition. Both technical challenges stipulated above need to be accounted for in a study of the fast transition. The objective of the research presented in this thesis aim to contribute to the understanding and the solution of the two main challenges facing the hydro power production. The goal and objectives of this thesis are as follows:

**The main goal** of the thesis has been to improve the fundamental understanding, and the numerical modeling, of transient operation of the RPT during different modes of operation. To accomplish this, the main goal are divided into three objectives:

- O1:** Investigate the difference between transient and steady state characteristic of a reversible pump-turbine model in four quadrants.
- O2:** Accomplish, and evaluate measurements of, a fast transition from pump to turbine mode of operation in a full scale power plant.
- O3:** Improve a numerical one-dimensional (1D) reversible pump-turbine model for transient simulation when the performance goes through all four quadrants in the characteristics.

## 1.4 Contributions

The research contributions published in the papers presented in Part II of the thesis can be summarized in the following points:

- The difference in steady state and transient characteristics in both pump and turbine mode of operation is explained by regarding the hydraulic inertia of the water masses in the system. This contribution is in accordance with **O1**.
- A modified Gibson method is proved to give a reliable flow measurements in a transient process in both pump and turbine mode of operation.
- A fast transition from pump to turbine mode of operation has successfully been proved in both model and prototype tests. This contribution is in accordance with **O2**.

- The pressure pulsations during the fast transition are compared to a normal procedure of change from pump to turbine mode of operation. This contribution is in accordance with **O2**.
- The fast transition is simulated using a 1D numerical model capable of simulating both pump and turbine mode of operation. The laboratory characteristics have been important in comparison to the improved 1D simulation model. The numerical and measured results show a good correlation, but requires further validation for RPTs with other geometries. This contribution is in accordance with **O3**.

## Chapter 2

# Theoretical background

---

■ This chapter give an introduction to reversible pump-turbines and their characteristics. The pressure pulsations of most concern during a transient operation and the connection between runner and system dynamics together with the use of one dimensional models to simulate this connection.

---

### 2.1 Introduction to reversible pump-turbines

The Francis type reversible pump-turbine, or more commonly; the reversible pump-turbine (RPT), is a hydraulic machine that can be used both to generate and store energy, by working either as a turbine or a pump depending on the rotational direction. The centrifugal pump and the Francis turbine have a similar runner design. The centrifugal pump in its modern form was introduced by John Appold in the mid 19<sup>th</sup> century. Around the same time the Francis turbine was developed by James B. Francis. The RPT builds on both the Francis turbine and the centrifugal pump.

Figure 2.1 show an illustration of a PSPP. The RPT is located between an upper and lower reservoir. The RPT illustration shows that the machine consists of (1) a spiral casing, (2) stay vanes, (3) guide vanes (GV), (4) runner blades, (5) impeller, (6) shaft, and (7) draft tube. It can generate electricity in turbine mode of operation, and pump water from the lower to the upper reservoir in pump mode of operation.

The RPT come in a wide range of designs adopted for different heads and flow

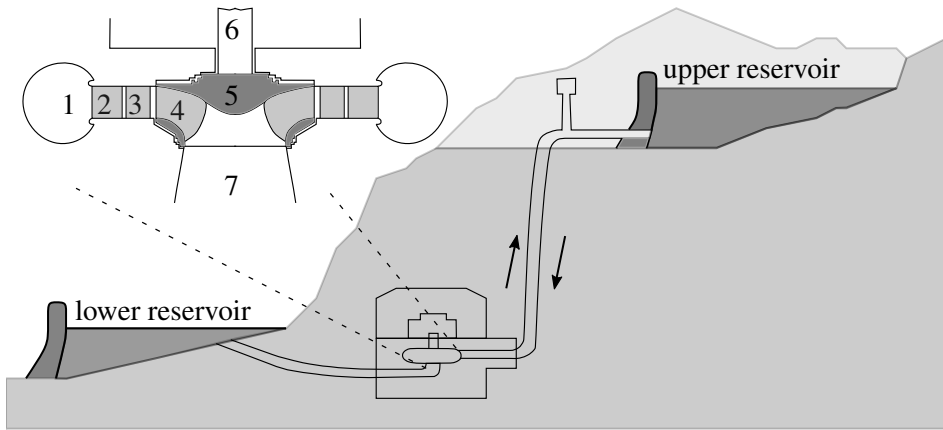


**Figure 2.1:** Detail of pump-turbine with system, consisting of: (1) the spiral casing, (2) stay vanes, (3) guide vanes, (4) runner blades, (5) runner, (6) the shaft and (7) the draft tube.

rates. Figure 2.2 show how the design changes depending on the specific speed, and is remade based on Hasmatuchi [5]. The specific speed is defined in Equation 2.3 [6].

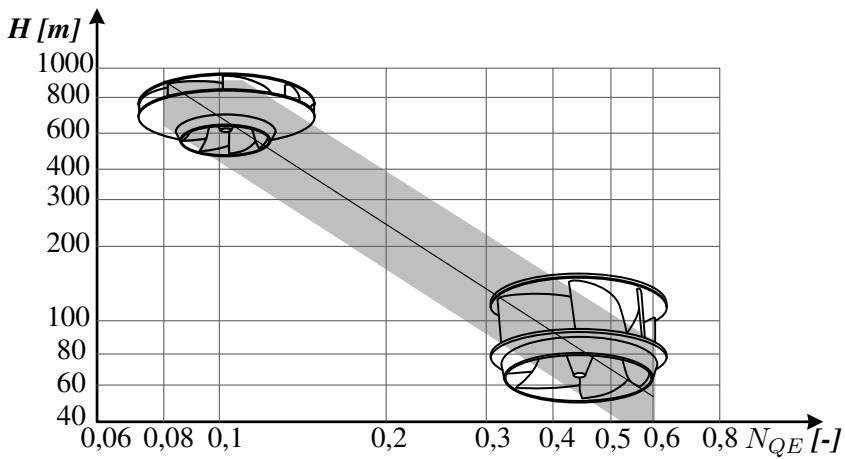


**Figure 2.2:** RPT runner shape by specific speed ( $N_{QE}$ ) and head ( $H$ )

## 2.2 Characteristics of reversible pump-turbine

The RPT might both intentionally, i.e. start up or load rejection, or by accident, i.e. electrical or mechanical failure, end up outside the normal areas of operation, marked in grey in Figure 2.3. As stated in IEC 60193: *"..it is also important to know its complete characteristics covering possible operating conditions outside the normal operating range"* [6]. An increase in start and stop operations, together with more off load operation will increase fatigue on the machine, as Seidel shows for Francis turbines [7]. Both a start up sequence or a load rejection in turbine mode an RPT may enter into reverse pump mode. Knowledge of the characteristics of the machine will help in the production planning to reduce the risk of entering into unstable areas, as such instability is damaging to both the machine and penstock as shown from prototype measurements by Walseth [8].

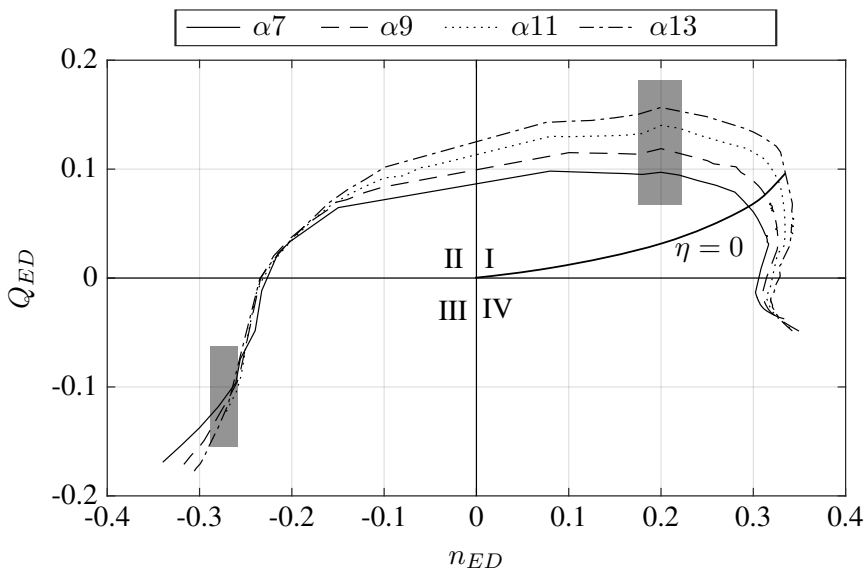


**Figure 2.3:** The four quadrant characteristics of a reversible pump-turbine for different GV opening degrees, area of normal operation marked in grey.

The wide area of operation for an RPT is often depicted in a four quadrant characteristic as seen in Figure 2.3.  $Q_{ED}$  and  $n_{ED}$  is the discharge and the speed factor. In accordance with IEC standard [6] they are described in Equation 2.2 and 2.1, respectively. The direction of discharge and speed is positive in turbine mode of operation.

$$n_{ED} = \frac{nD_2}{\sqrt{gH}} \quad (2.1)$$

$$Q_{ED} = \frac{Q}{D_2^2 \sqrt{gH}} \quad (2.2)$$

$$N_{QE} = n_{ED} Q_{ED}^{0.5} \quad (2.3)$$

**Quadrant I - turbine and turbine brake mode:** Turbine mode of operation is the area in Figure 2.3 where both the speed and discharge factor are positive and the RPT generates power. The normal operation in turbine mode is a small area around BEP, marked in grey in the figure. In turbine operation the flow goes from the high pressure side to the low pressure side through the RPT.

Below the zero efficiency line ( $\eta = 0$ ) in quadrant I, the RPT need a power input to operate. The area, known as turbine brake mode is often an unstable area, and well outside of normal operating procedures. The discharge and speed have the same direction as in turbine mode, but the reduced speed is higher than what the RPT will reach from available hydraulic pressure alone. The generator will need to deliver energy to the machine to surpass the zero efficiency line in a steady state situation. The deliberate operation below the zero efficiency line mostly occurs in the laboratory. With a prototype, turbine brake mode is entered into in a transient situation caused by the rotating inertia.

**Quadrant II - pump brake mode:** Pump brake mode is also an area well outside of normal operation. Here, the RPT will have a negative speed as shown in Figure 2.3. Even though the rotational speed is negative, it is not high enough to actually pump. So the discharge is still positive, going from the high to low pressure side through the RPT.

**Quadrant III - pump mode:** With both discharge and speed in negative direction, the RPT is in pump mode of operation. The discharge goes from the lower reservoir to the upper as it is pumped by the machine. There is need for energy input to operate in this area. As with the turbine mode of operation, it is only a small part of this quadrant that is considered as normal operation.

**Quadrant IV - reverse pump mode:** The negative discharge with high positive speed will give a mode of operation where the machine pumps water from lower to higher reservoir even though the machine rotates in turbine direction. This area is never intentionally entered into in normal operation of an RPT due to the damage it can cause both the machine and penstock.

### 2.2.1 Off-design conditions

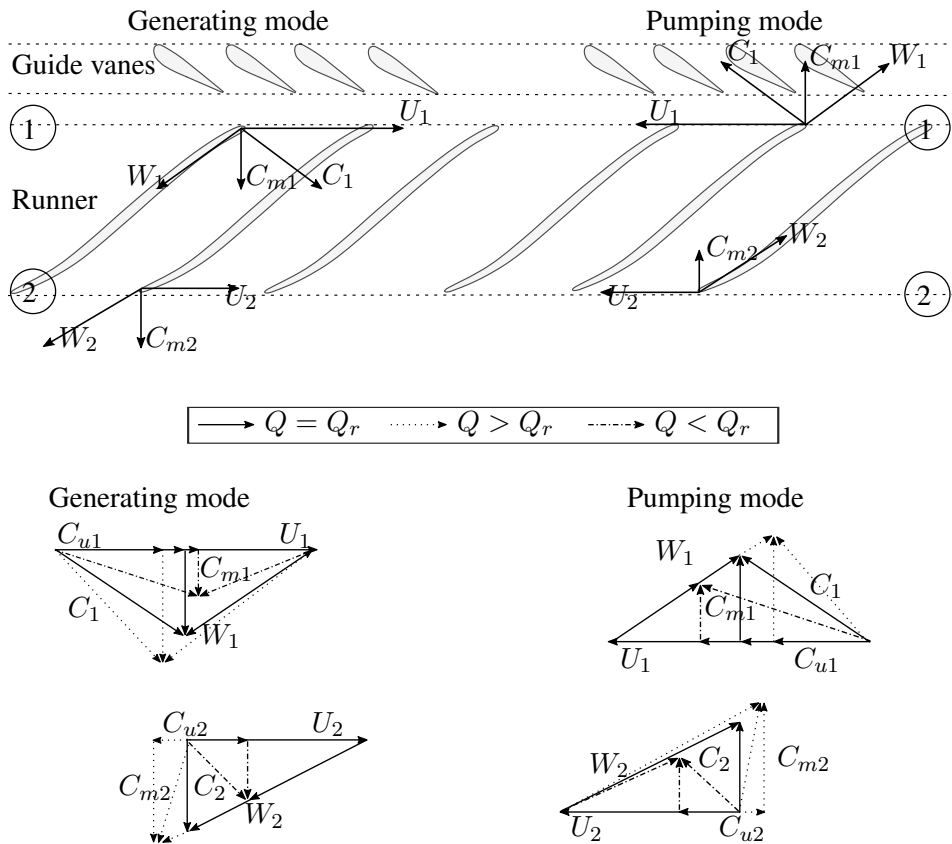


**Figure 2.4:** Blade-to-blade view of the runner with velocity triangles

Most areas in the full characteristics are seen as off-design conditions, where the inflow angle to the runner deviate from the ideal flow angle and the corresponding flow pattern at the outlet is decidedly nonuniform with occurrences of swirl, flow separation and backflow [7].

**Turbine part load operation** is the operation in turbine mode with a reduced guide vane opening. The theoretical velocity diagram for this operation is shown in Figure 2.4 where  $Q < Q_r$ . Seidel [7] describes the fluids tendency to flow towards the outer edges of the machine, resulting in backflow in the center of the draft tube and the development of swirl and periodic pressure pulsations. During

deep part load operation more stochastic pressure pulsations occur, and cavitation can also appear. Zhang [9] document the increasing amplitude of the pressure pulsations in a prototype RPT, with deeper part load operation. **Turbine full load operation** is achieved by opening the guide vanes beyond the ideal opening degree, resulting in the velocity diagram in Figure 2.4 where  $Q > Q_r$ . The fluid in full load operation flows more towards the axis of the machine [7]. Cavitation and pressure pulsations can be present, but are not as pronounced as in part load operation. The torque on the guide vanes is higher than at BEP, but still less than for the deep part load, as shown by Dörfler [10]. At **pump part load** the machine also experiences nonuniform flow streams, causing increased pressure pulsations [10].

The RPT also have two unstable areas in the characteristics. In quadrant I and IV, with positive speed, the **S-shaped characteristics** or **S-curve** as it is also called, is located in the transitional zone between turbine mode of operation and reverse pump mode. Due to the RPTs instability in the area, and the challenges it can cause during synchronization or load rejection of the machine, it is extensively researched [11]. Focusing on the flow characteristics during the S-curve; Hasmatuchi [5] showed the increased backflow and development of a stall cell as the RPT move from turbine brake to reverse pumping mode. In quadrant III, with negative speed, the **hump instability region** or **saddle instability** is characterized by the sudden drop in head, along with development of unsteady pressure pulsations due to back flow [9].

The last off-design part of the characteristics is the **pump brake mode**, quadrant II. With the objective to research a fast transition from pump to turbine (**O2**), this area is also entered into. In a laboratory experiment [12] and CFD simulations [13, 14] the pressure pulsations are shown to be higher than in other off-design conditions, not comparing the results to the s-shaped instability. However, the experimental data show that a faster passing time through quadrant II, results in lower pressure amplitudes in the area [12]. A reduction in the GV opening also seem to reduce the pressure amplitudes in pump brake mode [14].

## 2.2.2 System influence on characteristics

The first description of the full four quadrant characteristics were done on centrifugal pumps. Because of the similarities between the centrifugal pump and the RPT they are applicable to the understanding of reversible pump-turbine characteristics. Knapp investigated the connection between the steady state and dynamic characteristics as early as 1937 [15]. Through laboratory measurements, the full characteristics of a centrifugal pump were mapped out. Knapp assumed that *"..the instantaneous performance of the machine for any given set of momentary conditions occurring during a transient is identical with the steady-state perform-*

*ance for the same operating conditions.*" Following this assumption it is implied that *"..the accelerating forces exerted on the fluid within the machine during the transient are small in comparison to the forces required for normal steady state operation."* Even though the assumptions made by Knapp later are shown to be inaccurate, as will be discussed in Section 2.2.2, the characteristics give a good understanding of the conditions during different operational modes and the relationship between flow rate, rotational speed and torque. The experimental data provided by Knapp was also used by Stepanoff [16] to further explain the different modes of operation for centrifugal pumps.

The S-shaped characteristic is often described as unstable, but in fact a characteristic can not be unstable by itself. It is the interaction between the hydraulic system and the machine that can result in instabilities [17]. This is also shown by the different approaches to mitigate the instability at runaway speed for RPTs, where the method of misaligned guide vanes [18] and throttling the main inlet valve during start up [19] are both methods to influence the system, resulting in an increased stable operating zone.

In numerical simulation, the accuracy of the modeled waterway plays an important role in the correct representation of the characteristics. By including the inertia of the rotating masses within the machine in Nielsen's simulations, correctly represent the dampened oscillations around runaway speed for a scenario of load rejection in a Francis turbine [20].

## 2.3 One dimensional transient simulation

It is beneficial to be able to predict the hydraulic transients, in both machine and system, in an effective manner. A 1D model is both efficient and easy to implement. The difficulty lies in the representation of the hydraulic machine. With available experimental data, Suter curves can be used [21]. If experimental data isn't available however, a suitable model must be used. For hydraulic machines, the two most important properties to model correctly is the hydraulic torque and head acting on or being delivered by the machine [22].

Nielsen developed a set of Francis turbine equations based on the Euler equations, where the characteristics were based on the inlet and outlet dimensions [20]. In short form, they can be seen as Equation 2.4 and 2.5. The momentum equation 2.4, describe the change of flow rate through the RPT. The system head  $h$  is the head over the RPT and the  $h_{RPT}$  describe the dissipation or generation of head in the machine. The torque equation, Equation 2.5, describe the change in rotational speed dependent on the torque, where  $\tilde{T}_{RPT}$  hydraulic torque and  $\tilde{T}_g$  is the generator torque.

$$T_w \frac{dq}{dt} = h - h_{RPT} \quad (2.4)$$

$$T_a \frac{d\tilde{\omega}}{dt} = \tilde{T}_{RPT} - \tilde{T}_g \quad (2.5)$$

The model was later modified to include a pumping effect in the momentum equation, see Equation 2.6, and the result was a set of equations applicable for an RPT in turbine mode of operation, including the s-curve and reverse pumping [23]. The RPT model was further improved by Walseth, who introduced the pumping effect in the torque equation as well, see Equation 2.7 [8]. The study presented herein contains the first investigation of the model in a full, four quadrant characteristic.

$$T_w \frac{dq}{dt} = h - \frac{q|q|}{\kappa^2} - \sigma \left| \tilde{\omega}^2 - 1 \right| - \sigma \tilde{\omega}^2 + r_q \tilde{\omega} |q| \quad (2.6)$$

$$T_a \frac{d\tilde{\omega}}{dt} = q(qm_s - \psi \tilde{\omega} + \sigma \tilde{\omega} - r_q q) - r_m \tilde{\omega} |\tilde{\omega}| - \tilde{T}_g \quad (2.7)$$

All parameters are listed in Table 2.1 and are further defined as:

$$\tilde{\omega} = \frac{\omega}{\omega_r} \quad \psi = \frac{\omega_r^2 r_2^2}{gH_r} \quad \sigma = \frac{\eta_r - \psi}{\eta_r + \psi}$$

$$r_q = \frac{Q_r \omega_r}{gH_r} \left( \frac{r_1}{A_1 \tan \beta_1} - \frac{r_2}{A_2 \tan \beta_2} \right)$$

$$m_s = \frac{\omega_r Q_r}{gH_r} \frac{r_1}{A_1 \sin \alpha_r \kappa} (\cos \alpha + \sin \alpha_r \tan \alpha_r)$$

**Table 2.1:** Simulation model parameters

Parameter	Description	Unit
$\beta_1$	Inlet angle runner	[°]
$\beta_2$	Outlet angle runner	[°]
$\eta$	Efficiency	[-]
$\kappa$	Opening degree	[-]
$\omega$	Rotational speed	[s <sup>-1</sup> ]
$\tilde{\omega}$	Reduced $\omega$	[-]
$\psi$	Reduced geometric parameter	[-]
$\rho$	Density	[kg m <sup>-3</sup> ]
$\sigma$	Parameter with $\eta$ and $\psi$	[-]
$A_1$	Inlet area	[m]
$A_2$	Outlet area	[m]
$H$	System head	[m]
$h$	Reduced $H$	[-]
$m_s$	Reduced starting torque	[-]
$Q$	Flow rate	[m <sup>3</sup> s <sup>-1</sup> ]
$q$	Reduced $Q$	[-]
$r_1$	Inlet radius	[m]
$r_2$	Outlet radius	[m]
$r_m$	Disk friction constant	[-]
$R_q$	Geometrical parameter	[m <sup>-1</sup> ]
$r_g$	Reduced $R_q$	[-]
$\tilde{T}_m$	Reduced generator torque	[-]
$T_a$	Time constant, rotating inertia	[-]
$T_w$	Time constant, hydraulic inertia	[-]



# Chapter 3

## Research methods

---

■ This chapter presents the method and setup for both the laboratory and prototype measurements. It explains the basis for the Rainflow counting method, used in analyzing the pressure data from the experiments. Last, the equations used for the 1D simulation of the fast transition are presented.

---

The **fast transition** is a method to change from pump to turbine mode of operation, using the head to change the direction of the RPTs rotational speed from pump to turbine direction. The procedure start in normal pump mode of operation and end at idle speed in turbine mode of operation. To start the fast transition the generator torque is removed by disconnecting the machine from the grid, with guide vanes and main valve open. The disconnected generator result in the head being the only force affecting the speed of the RPT. Therefore the operational mode will naturally change from pump to turbine, through the forces acting on the RPT from the water. The fast transition is researched through laboratory and prototype measurements, and modeled using 1D simulation.

### 3.1 Laboratory measurements

Transient experiments like the fast transition are sensitive to the system, i.e the piping and other elements in the waterway between the upper and lower reservoir. To limit the disturbances during the experiment from the feeding pumps, the tests were run in an open loop configuration. The open loop ensures that the only forces

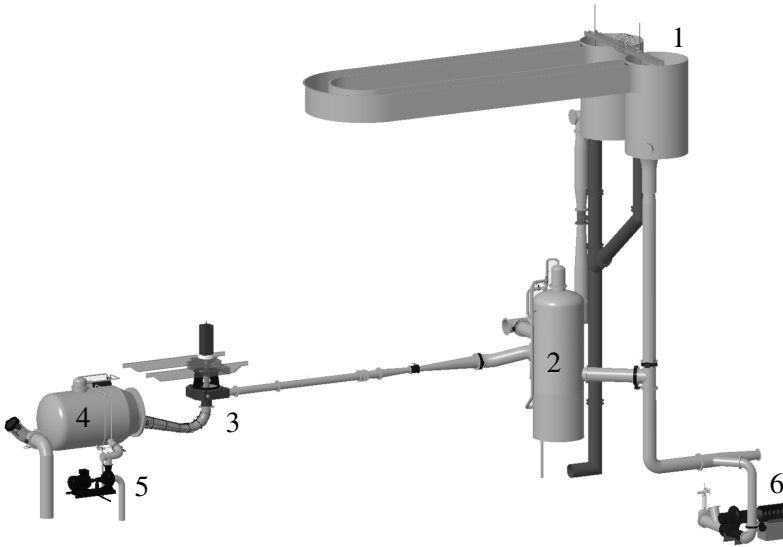


**Figure 3.1:** Hydraulic loop of the model pump-turbine

**Table 3.1:** Geometrical and operating parameters of the laboratory model pump-turbine

$D_1$	$D_2$	$B_1$	$n_{ED}^*$	$Q_{ED}^*$	$H^*$	$\beta_1$	$\beta_2$	$\alpha^*$
0.631 m	0.349 m	0.059 m	0.133	0.223	29.3 m	12°	12.8°	10°

present in the test loop come from the head, friction, hydraulic inertia and the RPT.

As seen in Figure 3.1 the upper reservoir has a constant head regulated by an overflow valve (1) and fed by a centrifugal pump (6). Upstream the RPT (3) there is a pressurized tank (2) like an air cushion. The draft tube ends up in an outlet tank (4), and the tank's water level is held constant by another centrifugal pump (5). In order to disconnect the hydraulic inertia of the outlet system a weir is installed in the outlet tank. The head is defined as the total energy difference between inlet of the turbine and outlet of the draft tube according to the convention. Geometrical and operating parameters of the investigated pump-turbine are presented in Table 3.1 [24].

### 3.1.1 Transient flow rate measurement

To measure the discharge fast and with high accuracy, a modified pressure-time method was used. The modified pressure time method was used by Nielsen and later Walseth in turbine mode of operation [20, 8]. By measuring the pressure difference over a certain pipe length, the pressure difference can be used to calculate

the transient flow during the mode change, using the electromagnetic flow meter (EMF) as a verification of the flow at steady state, before the start time ( $t_s$ ) and end time ( $t_e$ ) of each transient sequence. The change in flow rate for each time step,  $\Delta Q_i$  is described in Equation 3.1 and Equation 3.2 shows the friction loss.

$$\Delta Q_i = \frac{A}{\rho L} \int_{t_{i-1}}^{t_i} (\Delta p + \zeta) dt \quad (3.1)$$

$$\zeta = kQ_i^2 \quad (3.2)$$

Where  $\zeta$  is the friction loss in the pipe section as described in Equation 3.2,  $k$  is the friction factor,  $\Delta Q$  is the change in flow in one time step.  $A$  is the cross sectional area and  $L$  is the length of the pipe section.  $\rho$  the water density and  $\Delta p$  is the differential pressure of the two pressure sensors.

The flow rate during the fast transition was obtained as follows:

- The flow rate,  $Q_{emf}$  at  $t_s$  and  $t_e$  was measured by the flow meter.
- The average friction factor for both the steady state before and after the FT time period, respectively  $k_s$  and  $k_e$  where  $k = \frac{\Delta p}{Q^2}$
- $k_s$  was used until the rotational speed changed direction, then  $k_e$  was used for the rest of the measurement.
- $\Delta Q$  was calculated by the pressure difference for each time step and  $Q_i = Q_{i-1} + \Delta Q_i$ .

### 3.1.2 Experimental procedure

The procedure consisted of first setting the required head in the upper and lower reservoir. Then the rotational speed in pump mode was adjusted and the system was given time to stabilize. The generator torque was disconnected, causing the hydraulic pressure to force the RPT from pump mode to turbine mode. The transient measurement end with turbine runaway speed. Measurements were performed for constant GV angle  $7^\circ$ ,  $10^\circ$  and  $13^\circ$ , for each GV the measurement was repeated seven times.

## 3.2 Prototype measurements

The prototype measurements were conducted at Tevla power plant. Tevla consists of two identical reversible pump turbines and has an installed capacity of

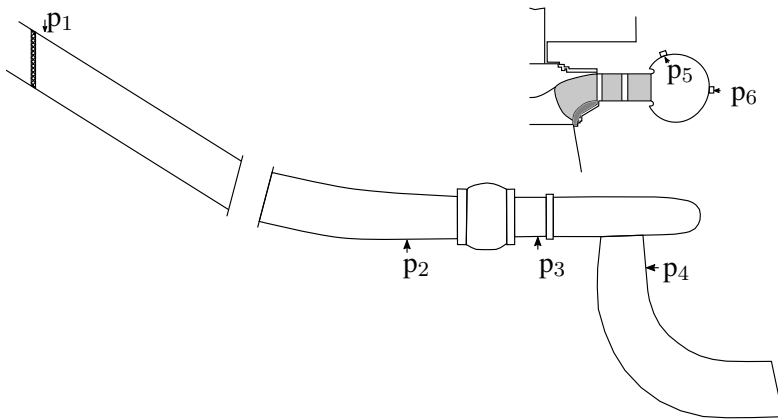


**Figure 3.2:** Illustration of instrument positions at Tevla

**Table 3.2:** Key parameters Tevla

$P$	$\alpha^*$	$\alpha_{idle}$	$H_{net}$
25 MW	53.9 %	14.7 %	148.4 m

2 · 25 MW. The power plant is located in the northern part of Trøndelag, a county in Norway, and is owned by Nord-Trøndelag Energi (NTE). The areas of investigation for the prototype measurements were the normal procedure (NP) and fast transition (FT) from pump to turbine mode of operation. One of the turbines was used in the experiment. During the experiment the other turbine was at standstill with the main inlet valve closed. Before measuring both the normal procedure and fast transition, reference values at BEP was measured. The sensor placement at Tevla was defined by existing pressure taps, which are shown in Figure 3.2.

### 3.2.1 Normal procedure

The normal transition procedure from pump to turbine is reached by first shutting down the machine in pump mode of operation and then carry out a normal start up in turbine mode of operation.

The procedure starts in normal pump mode of operation, after which the guide vanes and main valve are closed and the RPT is shut down. The shut down in pump mode is followed by an opening of the main valve and partially opening of the guide vanes. This allows the RPT to reach nominal speed at runaway. The generator is then synchronized and connected to the grid, and the guide vanes open further to desired operating point in turbine mode of operation.

### 3.2.2 Fast transition

The fast transition from pump to turbine also start in normal pump mode of operation. The guide vane angle is reduced from optimal pump opening to  $\alpha_{idle}$ , where  $\alpha_{idle}$  is the guide vane position that give idle speed at normal start up. After the adjustment of the guide vanes, the electric power to the generator is disconnected, in the same manner as in a load rejection scenario. Because of the pressure from the water masses the RPT will go from pump mode to runaway speed in turbine mode, and in the process pass through pump break mode. The RPT ends up at the ideal position to reconnect the generator to the grid.

The execution of the fast transition required operation of the power plant outside of normal procedures. Hence, a number of protection systems were shut off so as not to trigger the normal shutdown procedure if the power plant experience a load rejection. After which, the control system was switched to manual and the guide vanes were manually adjusted to  $\alpha_{idle}$ . Finally the main circuit breaker was turned, disconnecting the generator from the grid and leading to the fast transition. Due to the complexity of a modern power plant, a number of attempts were needed to find the correct method to bypass the fail-safes in the system. The end result was therefore one successful completion of the fast transition.

### 3.2.3 Rainflow counting method

The Rainflow counting method is a method to organize data with amplitudes. It most commonly used for stress data in preparation for the Miner's rule in a life cycle assessment [25]. The Rainflow method works just as well when analyzing pressure, and gives easy access to amplitude size and number of cycles. The method can also be used to sort the information by time, identifying when the amplitudes of interest occur.

The Rainflow method was introduced by Matsuishi and Endo [26], and gets its name from the association to the method of sorting the data with the flow of rain from a pagoda roof. The Rainflow method have been used to analyze pressure data as illustrated in Figure 3.3a. First the peaks and valleys are found as shown in Figure 3.3b. A section of the linearized peaks and valleys, where the time and pressure axis have been shifted, is shown in Figure 3.3c.

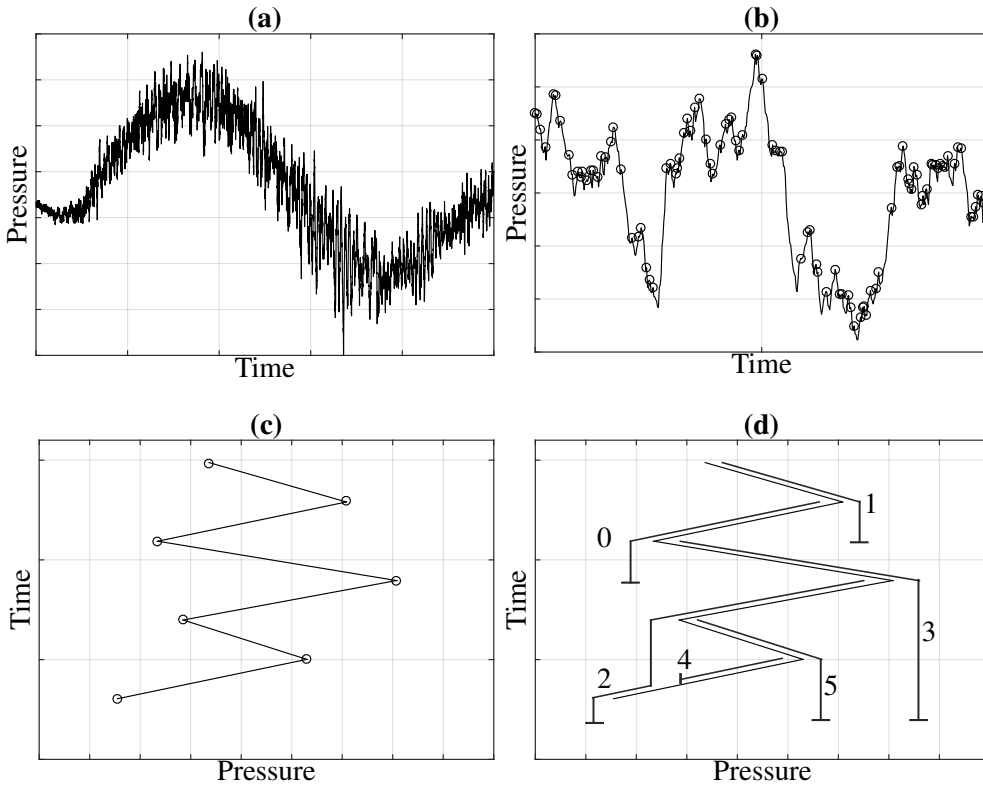


**Figure 3.3:** Illustration of steps in the Rainflow counting method

To count the amplitude cycles both by size and time of occurrence, the half cycles are categorized as in Figure 3.3d, following these rules:

- A half cycle ends when the peak on the other side have a greater magnitude (0 and 1).
- A half cycle ends when it reaches the end of the time line (2, 3 and 5).
- A half cycle ends when it meets another half cycle (4)

### 3.3 Transient simulation

The fast transition was simulated using MATLAB solver ode23s, and compared to the experiment presented in Section 3.1. The 1D simulation was implemented using a series of differential equations representing the RPT and the system. The RPT is described by the momentum equation in Equation 3.3, and the torque equation in Equation 3.4. The parameters are the same as shown in Section 2.3.

The simulation using the original equations (2.6 and 2.7) showed the need to improve the model in pump and pump brake mode of operation. The modified term is marked in Equation 3.3

$$T_w \frac{dq}{dt} = h - \frac{q|q|}{\kappa^2} - \overbrace{\sigma|\tilde{\omega}|\tilde{\omega}| - 1}^{\text{changed term}} - \sigma\tilde{\omega}^2 + r_q\tilde{\omega}|q| \quad (3.3)$$

$$T_a \frac{d\tilde{\omega}}{dt} = |q|(|q|m_s - \psi\tilde{\omega} + \sigma\tilde{\omega} - r_q|q|) - r_m\tilde{\omega}|\tilde{\omega}| - \tilde{T}_g \quad (3.4)$$

The system equations represent the laboratory setup presented in Figure 3.1. Equation 3.5 describes the change of reduced flow between the upper reservoir (1) and the pressure tank (2), Equation 3.6 describes the change of pressure in the pressure tank,  $h_{pt}$  (2), and Equation 3.7 describes the change in the flow through the hydraulic machine (3).

$$\frac{dq_1}{dt} = (h_1 - h_{pt}) \frac{1}{T_{w1}} \quad (3.5)$$

$$\frac{dh_{pt}}{dt} = (q_1 - q) \left( \frac{Q_r}{H_r A_{eq}} \right) \quad (3.6)$$

$$\frac{dq}{dt} = (h_{pt} - h_2 - h_{RPT}) \frac{1}{T_w} \quad (3.7)$$

where the reduced properties  $q$  and  $h$  are defined as

$$q = \frac{Q}{Q_r} \quad h = \frac{H}{H_r} = h_{pt} - h_2$$



## Chapter 4

# Summary of papers

---

■ In this chapter a summary of the papers are presented. The full papers can be found in Part II of the thesis and a shorter explanation binding the papers together with the objectives of this research can be found in Chapter 1

---

### **Paper 1 - Fast transition from pump to turbine mode of operation**

*M. F. Svarstad, T.K Nielsen* Published in International Journal of Fluid Machinery and Systems (IJFMS) 2018

The paper presents laboratory measurements of a fast transition from pump to turbine mode of operation on a reversible pump turbine. It gives a detailed description of the laboratory method used for conducting the experiment, with emphasis on the method to measure the flow rate in the transient operation. The difference in steady state and transient characteristics in both pump and turbine mode of operation is explained by regarding the hydraulic inertia of the water masses in the system. The paper is in accordance with the objective **O1** of the thesis.

### **Paper 2 - Pressure pulsations during a fast transition from pump to turbine mode of operation in laboratory and field experiment**

*M. F. Svarstad, T.K Nielsen* Published in (IOP) 2018

The paper presents a comparison of the fast transition conducted in laboratory and field experiments respectively. To evaluate the fast transition as stated in objective

**O2**, the focus in on the pressure pulsations measured during the fast transition. Even with differences both the RPTs geometry and system, clear similarities are found between the laboratory and field experiments.

### **Paper 3 - A comparison of pressure pulsations during normal and fast transition from pump to turbine mode of operation**

*M. F. Svarstad, T.K Nielsen* Submitted

To further evaluate the fast transition as stated in objective two, the pressure pulsations during the change from pump to turbine in both normal and fast transition are compared. The results show some high pressure pulsations in both transitional methods, where the fast transition exhibit the highest number of pressure pulsations. It is the normal procedure, however, who show the highest pressure amplitudes.

### **Paper 4 - Four Quadrant Characteristics Simulated with 1D RPT model**

*M. F. Svarstad, T.K Nielsen, P. T. Storli* Submitted

The paper presents simulated results of the fast transition, using a one-dimensional numerical pump turbine model. The simulated characteristics in both pump and turbine is compared to the laboratory measurements from **Paper 1**. The modification done to the model show a clear improvement to the original model. Where the modification give a better correlation to measurements.

## Chapter 5

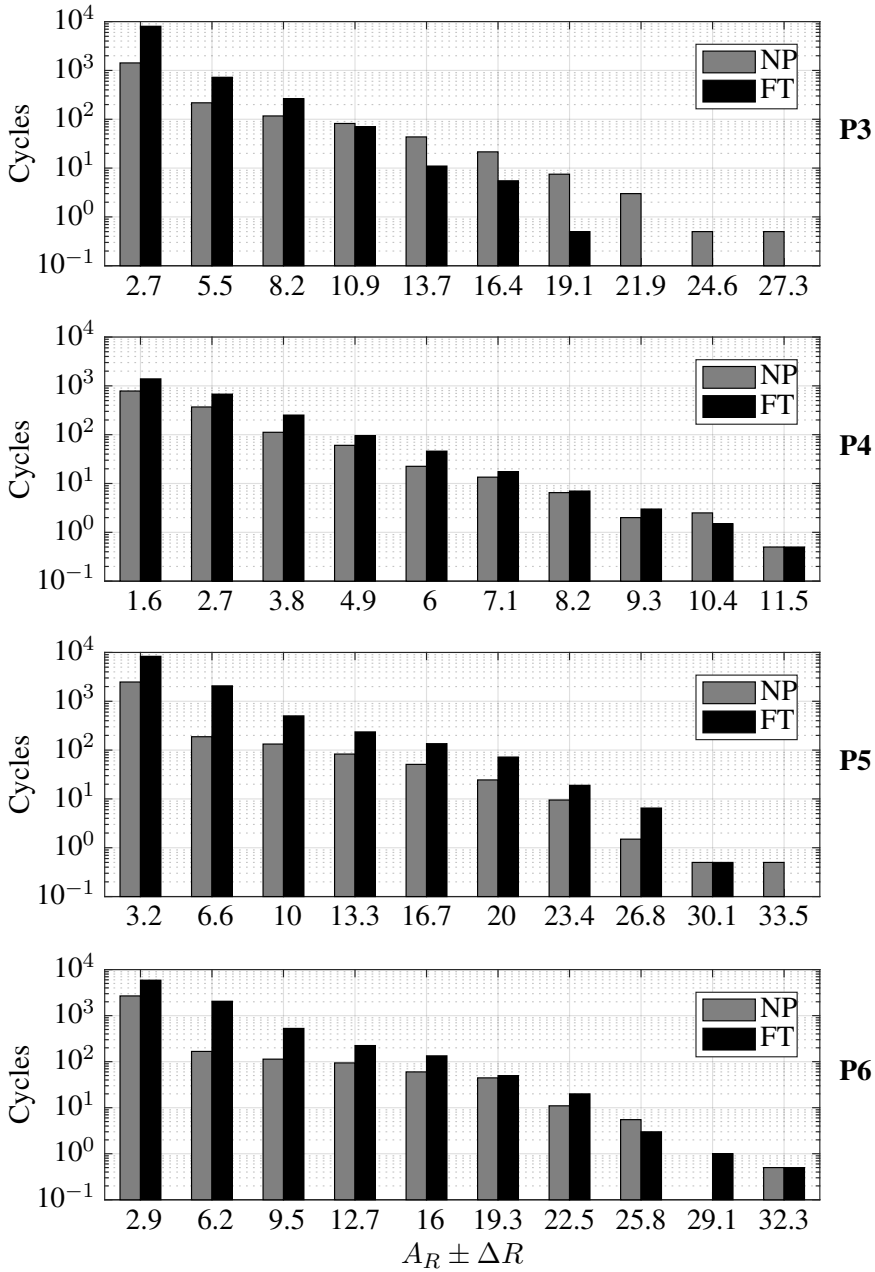
# General discussion

---

- This chapter first discuss the need for a fast transition in general term. Afterwards the prototype measurements and the simulation are discussed.
- 

The idea to use the fast transition to change from pump to turbine mode of operation is old; in a Norwegian pump power plant there already exists the control system to carry out the fast transition, even though it has never been tested. It is not surprising if similar systems exists in other power plants in Europe. Together with [12, 27, 13] the presented work is, however, the first scientific investigation into the fast transition. The value of the fast transition is closely connected to the other energy sources in the power market, the price fluctuations and how fast the power production response need to be to have a stable transmission grid. In Norway, with its high percentage of hydro power as the energy source, the need for the fast transition to balance the production to the demand is currently low. Since shifting demand for electricity can be met by changing the load in turbine mode of operation, we need to see a higher amount of export or a greater range in prices before it is viable for the Norwegian market. An energy system with a high amount of intermittent energy will benefit from the possibilities the fast transition of pump-turbines can deliver. In a future European energy market, the pump-turbine with fast transition can supply a needed balancing force.

## 5.1 Prototype measurements



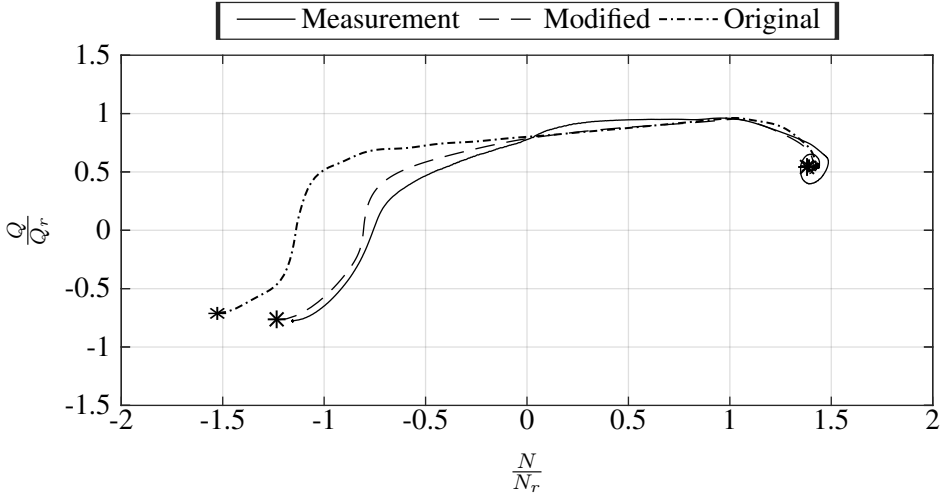
**Figure 5.1:** The number of cycles for all amplitudes ( $A_R$ ) during both the fast transition and normal procedure.  $\Delta R$  is 1.36, 0.57, 1.67 and 1.62 respectively for  $p_3$ ,  $p_4$ ,  $p_5$  and  $p_6$ .

Figure 5.1 show results from the measurements done at Tevla Power Plant presented in **Paper 3**. The position of the pressure sensors can also be found in Section 3.2. The difference in the amplitudes of the pressure pulsations for the fast transition compared to a normal procedure are small, as can be seen in Figure 5.1. The normal procedure has higher or equivalent maximum amplitudes for all sensors compared to the fast transition. The investigation indicated that the fast transition may indeed be a viable method. However, some factors need to be addressed.

First, there was no possibility to measure the pressure pulsations in the vaneless space. Since the normal procedure to stop the pump includes the closing of the guide vanes, some of the pressure pulsations measured in the normal procedure likely come from the closing of the guide vanes. The highest amplitudes in the normal procedure can thus be upstream the guide vanes, and not affecting the runner. While with the fast transition, the guide vanes are not closed and the runner will be affected by all the measured pressure pulsations. It is even likely that the amplitudes are higher than recorded, due to the rapid dampening of the amplitudes. The first limitation indicates that the runner experience higher amplitudes in the runner for the fast transition than the normal procedure.

Secondly, due to restrictions at the power plant, the fast transition had to be executed manually. The result is a slower fast transition than what could be achieved if the process was automatic. It also resulted in the need to reduce the guide vane opening while still connected to the grid in pump mode, before being able to turn of the main circuit breaker, disconnecting the generator. There is reason to believe that a fast transition where the guide vane opening is continually reduced while in the transient phase, as opposed to reducing the angle before the transition, would reduce the pressure amplitudes. The number of cycles would also decrease with an automated procedure. The second limitation indicates therefor that changes in the procedure in the fast transition can reduce the pressure pulsations.

## 5.2 Simulation model



**Figure 5.2:** Simulation of the fast transition using both the original and modified momentum equation, compared to measured characteristic

The change done to the existing numerical RPT model gave a good correlation to the measured characteristic, as can be seen in the comparison between the original and modified simulation in Figure 5.2. The change in the momentum equation resulted in a corresponding change in the torque equation, increasing the torque in pump mode of operation.

The four quadrant characteristics in a  $n_{ED}Q_{ED}$  diagram can be transposed to a  $QH$  diagram, normally used to describe the pump characteristics. By setting an arbitrary constant rotational speed ( $n$ ) and rearranging the Equations for  $n_{ED}$  and  $Q_{ED}$ , as in Equation 5.1 and 5.2, the head ( $H$ ) and flow rate ( $Q$ ) is found.

$$H = \frac{1}{g} \left( \frac{nD_2}{n_{ED}} \right)^2 \quad (5.1)$$

$$Q = Q_{ED} D_2^2 \sqrt{gH} \quad (5.2)$$

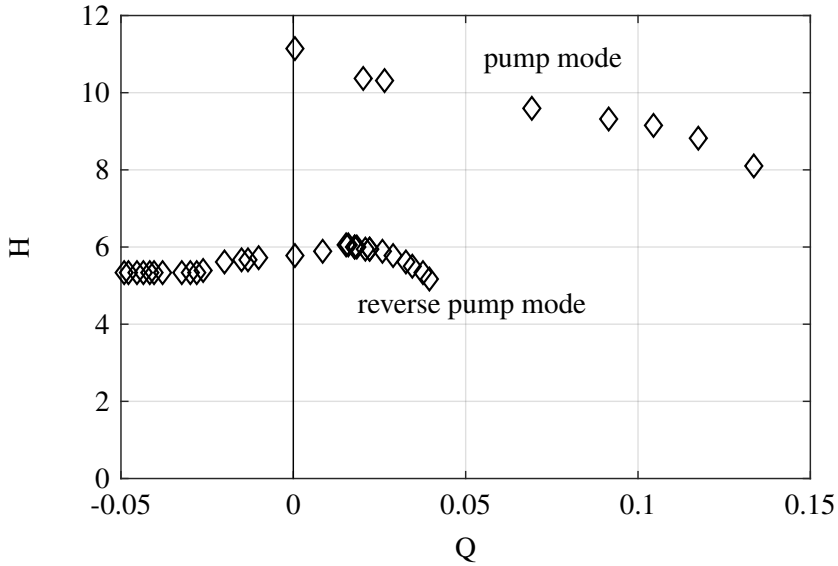


**Figure 5.3:** Transposed  $QH$  characteristics of a section of the four quadrant characteristics

The  $QH$  characteristics in Figure 5.3 show clearly the head difference between the reverse pump and pump mode of operation. This difference in head is represented by the changes in the momentum equation in the simulation model. In reality, the pumping in reverse pump mode can be seen as the pumping occurring with backwards bent blades, and it is natural that this will give a smaller lifting power than in pump mode, with the the correct blade curvature. The operation at off-design conditions, and especially in quadrant II and IV, result in a deviation between the design angles and the angles of the velocity vectors. Even though it is not possible to recreate the 3D, nonuniform flow pattern in a 1D model, the simulated velocity vectors needs to correspond to an averaged flow pattern resulting in the same flow rate and rotational speed as the measured characteristic. The averaged streamline pattern and its  $\beta$  angles should be studied further in the continuation to enhance the model.



## Chapter 6

# Conclusion

The main goal of the thesis has been to improve the fundamental understanding, and the numerical modeling, of transient operation of the RPT during different modes of operation.

From the laboratory measurements it is shown that the steady state and transient characteristics in both pump and turbine mode of operation is explained by regarding the hydraulic inertia of the water masses in the system. The laboratory measurements also prove that a modified Gibson method is a reliable method to measure the flow rate in a transient process, also when the flow change direction during the period.

This work presents the first documentation of a fast transition done at a full scale power plant. The fast transition from pump to turbine mode of operation has successfully been proved in both model and prototype tests. The comparison between pressure pulsations during the fast transition and the normal start and stop procedure show similar maximum amplitudes, with the maximum amplitudes for the normal procedure being marginally higher.

The fast transition is simulated using a 1D numerical model capable of simulating both pump and turbine mode of operation. The laboratory characteristics have been important in comparison to the improved 1D simulation model. The numerical and measured results show a good correlation, but requires further validation for RPTs with other geometries.



# Chapter 7

## Further work

Based on the discussion in Chapter 5 the following suggestions for further work are presented:

- Expand the investigation of the normal procedure to include vibration in the guide vanes to better be able to compare the two methods of transition from pump to turbine.
- Improve the method of fast transition with the adjustment of the guide vanes during the transient phase.
- Test the RPT equations by comparing the simulation results to other RPT models and GV openings.
- Study the possible impact the fast transition has on the stability at runaway speed.



# Bibliography

- [1] IPCC. *Global Warming of 1.5C*. Intergovernmental Panel on Climate Change (IPCC), 2018.
- [2] Vidkunn Hveding and Norges tekniske høgskole: Institutt for vassbygging. *Vannkraft i Norge*. Trondheim: Universitetet i Trondheim, Norges tekniske høgskole, Institutt for vassbygging, 1992. 83 pp.
- [3] T.M. Welte, E. Solvang and B. Børresen. “Analysing Changes to Operating Conditions at Norwegian Hydro Plants”. In: *International Journal on Hydropower and Dams* 17.1 (2010), pp. 61–66.
- [4] Arthouros Zervos, Christine Lins and Canadian Electronic Library (Firm). *Renewables 2018 Global Status Report*. 2018.
- [5] Vlad Hasmatuchi et al. “Experimental Evidence of Rotating Stall in a Pump-Turbine at Off-Design Conditions in Generating Mode”. In: *Journal of Fluids Engineering* 133.5 (7th June 2011), pp. 051104-051104-8.
- [6] IEC. *Hydraulic Turbines, Storage Pumps and Pump-Turbines - Model Acceptance Tests*. Technical Standard NEK EN 60193:1999. 1999.
- [7] U. Seidel et al. “Dynamic Loads in Francis Runners and Their Impact on Fatigue Life”. In: *IOP Conference Series: Earth and Environmental Science* 22.3 (1st Mar. 2014), p. 032054.
- [8] Eve Cathrin Walseth. “Dynamic Behavior of Reversible Pump-Turbines in Turbine Mode of Operation”. Trondheim: Norwegian University of Science and Technology, Faculty of Engineering Science and Technology, Department of Energy and Process Engineering, 2016.

- [9] Yuning Zhang et al. “Experimental Study of Load Variations on Pressure Fluctuations in a Prototype Reversible Pump Turbine in Generating Mode”. In: *Journal of Fluids Engineering* 139.7 (27th Apr. 2017), pp. 074501-074501-4.
- [10] Peter Dörfler, Mirjam Sick and André Coutu. *Flow-Induced Pulsation and Vibration in Hydroelectric Machinery: Engineer’s Guidebook for Planning, Design and Troubleshooting*. Springer Science & Business Media, 28th Aug. 2012. 257 pp.
- [11] Giovanna Cavazzini et al. “Analysis of the Unstable Behavior of a Pump-Turbine in Turbine Mode: Fluid-Dynamical and Spectral Characterization of the S-Shape Characteristic”. In: *Journal of Fluids Engineering* 138.2 (10th Sept. 2015), pp. 021105-021105-12.
- [12] O. Braun and N. Ruchonnet. “Analysis of Pressure Pulsations during the Fast Transition of a Pump Turbine from Pumping to Generating Mode”. In: *Journal of Physics: Conference Series* 813.1 (2017), p. 012017.
- [13] C Stens and S Riedelbauch. “Investigation of a Fast Transition from Pump Mode to Generating Mode in a Model Scale Reversible Pump Turbine”. In: *IOP Conference Series: Earth and Environmental Science* 49 (Nov. 2016), p. 112001.
- [14] C Stens and S Riedelbauch. “Influence of Guide Vane Opening on the Flow Phenomena in a Pump Turbine during a Fast Transition from Pump Mode to Generating Mode”. In: *Journal of Physics: Conference Series* 813 (4th Apr. 2017), p. 012024.
- [15] R. T. Knapp. “Complete Characteristics of Centrifugal Pumps and Their Use in the Prediction of Transient Behavior”. In: *Transactions of the ASME* (1937), pp. 683–689.
- [16] A. J. Stepanoff. *Centrifugal and Axial Flow Pumps: Theory, Design, and Application*. 2nd ed. New York: Wiley, 1957. vii+462.
- [17] Thomas Staubli et al. “Starting Pump-Turbines with Unstable Characteristics”. In: *Hydro 2010* (2010).
- [18] J T Billdal and A Wedmark. “Recent Experiences With Single Stage Reversible Pump-Turbines in GE Energy’s Hydro Business”. In: *Hydro 2007*. Granada, Spain, 2007.
- [19] P K Dörfler et al. “Stable Operation Achieved on a Single-Stage Reversible Pump-Turbine Showin Instability at No-Load”. In: *Proc. of 19th IAHR Symposium Hydraulic Machinery and Systems*. Singapore, 1998.

- 
- [20] Torbjørn K. Nielsen. “Transient Characteristics of High Head Francis Turbines”. Trondheim: Universitetet i Trondheim, Norges tekniske høgskole, Institutt for hydro- og gassdynamikk, 1990.
- [21] E Benjamin Wylie, Victor Lyle Streeter and Lisheng Suo. *Fluid Transients in Systems*. 1993.
- [22] Pål-Tore Storli and Torbjørn K. Nielsen. “Simulation and Discussion of Models for Hydraulic Francis Turbine Simulations”. In: *IFAC-PapersOnLine* 51.2 (2018), pp. 109–114.
- [23] Torbjørn K. Nielsen. “Simulation Model for Francis and Reversible Pump Turbines”. In: *International Journal of Fluid Machinery and Systems* 8.3 (2015), pp. 169–182.
- [24] Grunde Olimstad. “Characteristics of Reversible-Pump Turbines”. Trondheim: Norwegian University of Science and Technology, Faculty of Engineering Science & Technology, Department of Energy and Process Engineering, 2012.
- [25] Xin Liu, Yongyao Luo and Zhengwei Wang. “A Review on Fatigue Damage Mechanism in Hydro Turbines”. In: *Renewable and Sustainable Energy Reviews* 54 (Feb. 2016), pp. 1–14.
- [26] International Organization for Standardization. *ISO 12110-2:2013 - Metallic Materials - Fatigue Testing - Variable Amplitude Fatigue Part 2: Cycle Counting and Related Data Reduction Methods*.
- [27] N. Ruchonnet and O. Braun. “1D Simulation of Pump-Turbine Transition”. In: *Journal of Physics: Conference Series* 813.1 (2017).



**Part II**

**Papers**



# Paper 1

## **Fast Transition from Pump to Turbine mode of Operation**

Svarstad, M. F., Nielsen, T. K.

*International Journal of Fluid Machinery and Systems* vol. 11, 2018



**Original Paper**

# Fast Transition from Pump to Turbine Mode of Operation

Magni F. Svarstad<sup>1</sup> and Torbjørn K. Nielsen<sup>1</sup>

<sup>1</sup>Waterpower Laboratory, Norwegian University of Science and Technology  
Alfred Getz' v. 4, 7034 Trondheim, Norway, [magni.f.svarstad@ntnu.no](mailto:magni.f.svarstad@ntnu.no), [torbjorn.nielsen@ntnu.no](mailto:torbjorn.nielsen@ntnu.no)

## Abstract

The reversible pump turbine (RPT) is a suitable machine to control fluctuations in the energy market. The usage of RPTs for this purpose will increase the number of operational mode changes of the machine. In order to reduce the response time of the machine, fast transitions between the modes of operation are necessary. Therefore, increased knowledge of how the machine operates during these fast transitions is needed. This includes the investigation of the transient characteristics for the whole operating range of the machine. This paper presents experimental results from a fast transition from pump to turbine mode. The flow rate is measured by the use of a modified pressure time method. The resulting transient characteristics are compared with steady state characteristics. Experiments have been performed on a model scale reversible pump turbine in the Waterpower Laboratory at the Norwegian University of Science and Technology (NTNU). The results show that the pressure pulsations are highest at low discharge in both pump and turbine mode of operation and at runaway speed in turbine. Oscillations at runaway speed is reduced with lower opening degree on the guide vanes. The results also show a difference between the steady state and transient characteristics in the pump mode due to the inertia of the water masses.

**Keywords:** Reversible pump turbine, Transient operation, Mode change

## 1. Introduction

When discussing the future of the energy market, the reversible pump turbine (RPT) are often given the role of balancing the intermittent energy production. The introduction of intermittent renewable energy sources calls for a faster regulating force in the energy market. Balancing the energy production can be done by RPTs and require the machines to change the mode of operation more frequently. In such a scenario, the need is not only for an increase in operational mode changes, but also for a decrease in the transition time between the pump and turbine mode of operation.

In reversible pump turbines, as in Francis turbines, it is well documented that the machines experience high fatigue loads in off-design and start and stop operations [1]–[3].

For reversible pump turbines the instabilities that can occur during start up, both in pump mode [4] and turbine mode [5] are also areas where a lot of research is available.

There is, however, less information about the transition between the different operational modes. Early, and most well-known research on this topic is the four quadrant characteristics of a pump presented in [6] by Stepanoff. The experimental data describing the four quadrant characteristics in [6] was done by Knapp [7].

Ruchonnet and Braun [8] have presented transient characteristics from experimental research done from pump to turbine mode and from turbine to pump mode.

They refer to high-pressure pulsations during the transient period, and especially high amplitudes in energy dissipation mode. Stens and Riedelbauch [9] have investigated the same transient operation using Computational Fluid Dynamics (CFD). They conclude that the fast transitions lead to stall conditions between the guide vanes and vortices in the runner and draft tube, and that this is the cause of the off-design conditions in the runner. Liu et al. [10] have done CFD on a transient process caused by power failure from pump mode to turbine mode. The authors show that the minimum value for the transient head occurs when the flow rate is approximately zero, which means between energy dissipation mode and turbine mode of operation.

When connecting a hydraulic machine to the grid, the rotational speed of the machine have to be equal the synchronous speed. The most common way to achieve the correct rotational speed before connecting the machine to the grid is to let the machine rotate at runaway speed with a given opening of the guide vanes. It is therefore of interest to look closer at the systems behaviour at runaway speed after a fast transition from pump to turbine mode of operation.

This article investigates the transient characteristics of a reversible pump turbine, from pump to turbine mode of operation. An important part of the work has been the development of a reliable method to measure the flow rate in this scenario. The method of measuring the flow rate, together with the resulting transient characteristics, are presented in the article. The transient characteristics are also compared to the steady state characteristics for the same machine.

## 2. Experimental setup

When doing transient experiments it is important to remove disturbances on the system caused by the pump, if run in closed loop. The Francis test rig was therefore arranged to operate in an open loop configuration when testing the reversible pump turbine. As seen in Fig. 1 the upper reservoir have a constant head regulated by an overflow valve (1) and fed by a centrifugal pump (6). Upstream the turbine (3) there is a pressurized tank (2) with an air cushion. The draft tube ends up in an outlet tank (4), and the tanks water level is held constant by another centrifugal pump (5). In order to disconnect the hydraulic inertia of the outlet system a weir is installed in the outlet tank. The head is defined as the total energy difference between inlet of the turbine and outlet of the draft tube according to the convention as seen in eq. (1).

**Table 1** RPT runner parameters

$D_1$	$D_2$	$B_1$	$n_{ed}$	$Q_{ed}$	$H^*$	$B_{hp}$	$B_{lp}$	$\alpha^*$
0.631 m	0.349 m	0.059 m	0.133	0.223	29.3	12°	12.8°	10°

The model runner is designed by Grunde Olimstad [11] during his PhD work. The laboratory set-up is, with some modifications, the same as used by Eve Walseth as part of her PhD thesis [12]. The runner parameters are listed in Table 1.

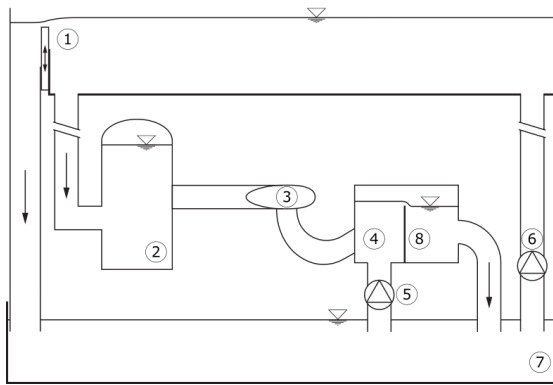


**Fig. 1** The open loop configuration of the Francis test rig with; upper reservoir (1), pressure tank (2), RPT (3), draft tube tank (4), downstream feeding pump (5), upstream feeding pump (6), main water reservoir (7) and weir in draft tube tank (8)

### 2.1 Instrumentation

Flow rate, torque, rotational speed and pressure were measured during the experiment. Table 1 lists the different sensors, and details for each instrument used indicate the placement of each instrument. The head calculated as shown in eq. (1). The sample rate of 5000 Hz was used.

**Table 2** Instrument details

<i>Abbreviation</i>	<i>Description</i>	<i>Sensor Type</i>	<i>Location</i>
$p_{i1}$	Inlet pressure	Druck UNIK 5000	Turbine inlet
$p_{i2}$	Upstream inlet pressure	Druck UNIK 5000	Inlet pipe
$P_{v1}$	Vaneless space pressure	Kulite	Vaneless space
$P_{dt}$	Draft tube pressure	Kisler	Draft tube upper
$P_o$	Outlet pressure	PTX	Draft tube lower
$M$	Torque	Hottinger	Main shaft
$Q_m$	Electromagnetic flowmeter	Krohne	Inlet pipe
$n$	Rotational speed	Encoder	Generator draft

$$H = \frac{p_{i1} - p_o}{\rho g} + \frac{Q_g^2}{2g} \cdot \left( \frac{1}{A_{i1}^2} - \frac{1}{A_o^2} \right) \quad (1)$$

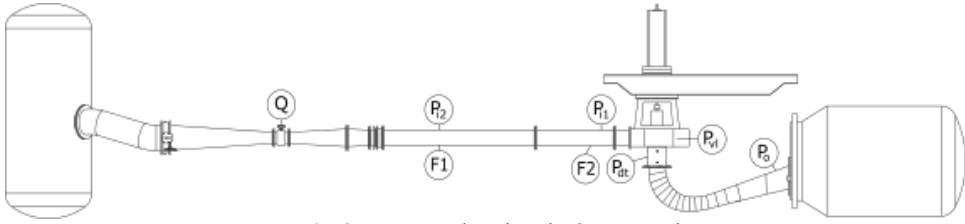


Fig. 2 Instrument locations in the test section

## 2.2 Transient flow rate measurement

To measure the discharge fast and with high accuracy, a modified pressure-time method was used. The pressure-time (Gibson) method referred to in IEC 60193 [13] is used for measuring the initial flow using the transient pressure difference as the guide vanes closes to zero opening. In this experiment however, a modified pressure-time method was used. By measuring the pressure difference over a certain pipe length, the pressure difference can be used to calculate the transient flow during the mode change, using the electromagnetic flow meter (EMF) as a verification of the flow at steady state, both at the start and the end of each transient sequence. Nielsen [14] was the first to use the pressure-time method to find the flow at each increment of time in a transient sequence, while doing tests in the turbine mode of operation.

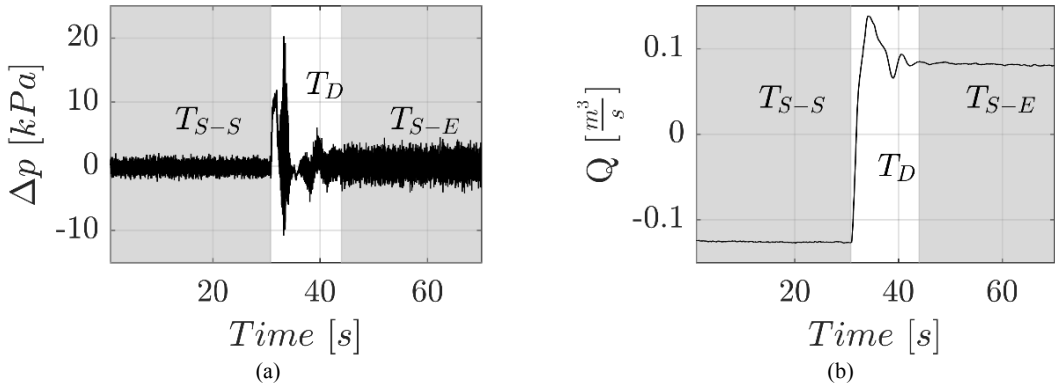


Fig. 3 The differential pressure  $\Delta P$  (a) used to calculate the flow  $Q$  (b) where the steady state area at start and end are given by the EMF

Figure 3(a) shows the measured differential pressure between two pressure sensors ( $p_{i1}$  and  $p_{i2}$ ) with a distance of 5.345 m, and with a constant cross sectional area between them. The transient flow rate as seen in Fig. 3(b) is found by integrating the pressure difference in accordance with the pressure-time method as stated in eq. (3) and eq. (4),

$$\Delta Q_i = \frac{A}{\rho L} \int_{t_{i-1}}^{t_i} (\Delta p + \zeta) dt \quad (2)$$

$$\zeta = kQ^2 \quad (3)$$

where  $\zeta$  is the friction loss in the pipe section,  $k$  is the friction factor,  $\Delta Q$  is the change in flow in one time step.  $A$  is the cross sectional area and  $L$  is the length of the pipe section.  $\rho$  is the water density and  $\Delta p$  is the differential pressure of the two pressure sensors. Each measurement is divided into three parts.  $t_0 \leq T_{S-S} < t_1$  is the time period from the start of the steady state measurement up to the start of the transient period.  $t_1 \leq T_D < t_2$  is the transient period where the RPT changes from pump to turbine mode of operation.  $t_2 \leq T_{S-E} < t_3$  is the steady state period from the end of the transient measurement to the end of the measurement.

The flow rate in the transient section  $Q_g$  was obtained as follows:

- The flow rate,  $Q_m$  at  $T_{S-S}$  and  $T_{S-E}$  were measured by the flow meter.
- The average friction factor for the time period  $T_{S-S}$ ,  $k = \frac{\Delta p_{T_{S-S}}}{Q_{T_{S-S}}^2}$
- The friction loss was found at  $T_{S-S}$  and  $T_{S-E}$  using the relationship given in eq. (3).
- $\zeta_{T_{S-S}}$  was used until the rotational speed changed direction, then  $\zeta_{T_{S-E}}$  was used for the rest of the measurement.
- $\Delta Q$  was calculated by the pressure difference for each time step and  $Q_i = Q_{i-1} + \Delta Q_{g_i}$

## 2.2 Experiment procedure

The procedure consisted of first setting the required head in the upper and lower reservoir. Then the rotational speed in pump mode was adjusted and the system was given time to stabilize. The generator torque was disconnected, causing the hydraulic pressure to force the RPT from pump mode to turbine mode. The transient measurement ended at turbine runaway speed. Measurements were performed for constant guide vane angle (GV) 7°, 10° and 13°, for each GV the measurement was repeated seven times.

## 3. Results

### 3.1 Transient characteristics

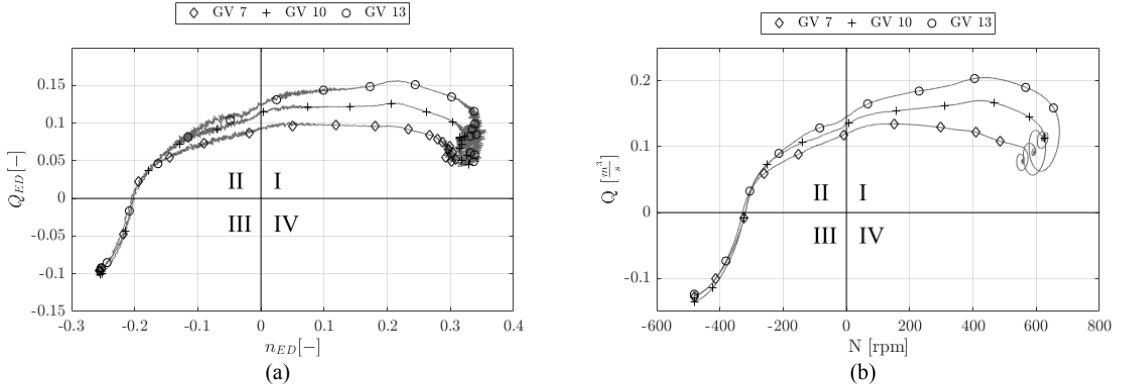


**Fig. 4** Transient measurements for three different guide vane openings in non-dimensional (a) and physical (b) units. I is turbine mode, II is dissipation mode, III is pump mode and IV are reverse pump mode.

The four quadrant, transient characteristics for three different guide vane openings are presented in Fig. 4, shown as machine characteristics Fig. 4(a) and system characteristics Fig. 4(b). Machine characteristics have non-dimensional units  $Q_{ED}$  and  $n_{ED}$  as defined in eq. (4) and eq. (5). The non-dimensional units are independent of both the system around the machine and the dimensions of the machine parameters.

$$Q_{ED} = \frac{Q}{D^2 \sqrt{gH}} \quad (4)$$

$$n_{ED} = \frac{nD}{\sqrt{gH}} \quad (5)$$

In Fig. 4(b) the different guide vane openings give a similar flow rate per rotational speed in pump mode (III). When the flow changes direction in quadrant II the effect of the guide vane positions becomes apparent. Finally, in turbine mode of operation the result of an increased guide vane opening can be seen giving an increased spiral around the runaway position.

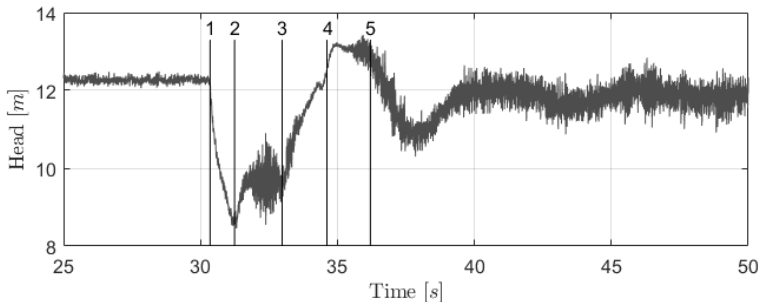


**Fig. 5** The change in head (H) during the transient experiment. The numbering show start of  $T_D$  (1), flow rate zero (2), rotational speed zero (3), flow rate maximum (4), rotational speed maximum (5).

The pressure oscillations in the system can be seen in Fig. 5 and show the changes in head over time. Since the transient measurements shown in Fig. 4(a) include H, the same oscillations can be seen in this figure. The highest oscillations are found in the dissipation mode in quadrant II and at turbine runaway in quadrant I. All of the guide vane openings show similar magnitude in the oscillations in dissipation mode. At runaway speed the oscillations increase with increasing opening.

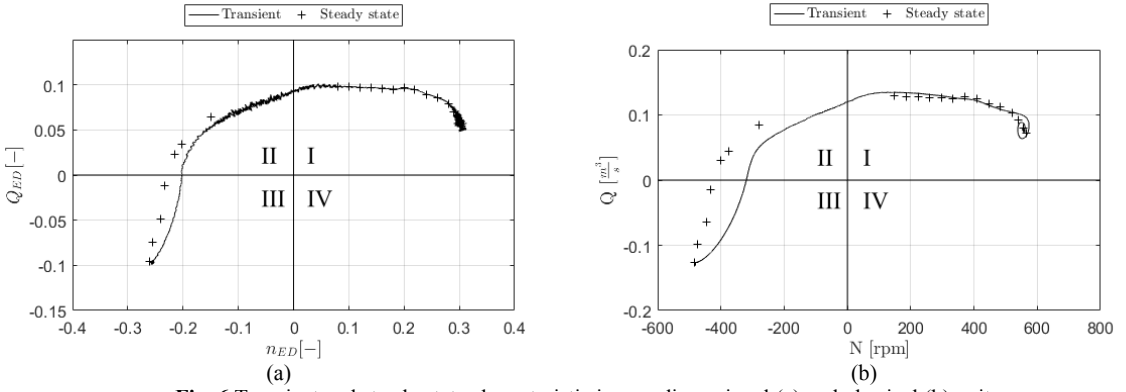


**Fig. 6** Transient and steady state characteristic in non-dimensional (a) and physical (b) units

Figure 6 compare the transient measurement with steady state measurements. Figure 6(b) has two areas where the transient and steady state measurements differ significantly, when the rotational speed is negative and around runaway speed. In Fig. 6(a) the difference are concentrated in quadrant II and III.

The difference between the steady state and transient measurements in turbine mode of operation has been addressed by Nielsen [14]. By removing the inertia of the water masses as in eq. (6) when calculating the head, he showed that the transient and steady state characteristics becomes equal around runaway speed.

$$H_t = H - I \frac{dQ}{dt} \tag{6}$$

$$I = \sum \frac{A}{gL}$$

In eq. (6) H is the measured head, I is the hydraulic inertia,  $dQ/dt$  is the change in flow rate over time and  $H_t$  is the transient head. A and L is the cross-sectional area and the length of the pipe segment respectively.

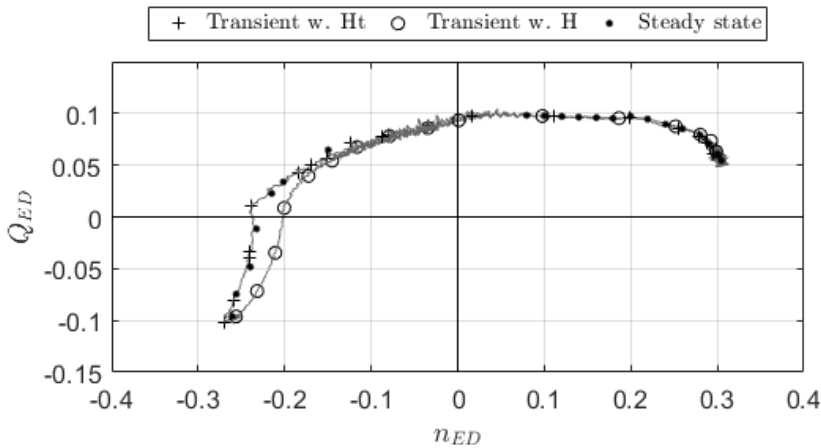


**Fig. 7** The difference between the measured transient characteristics with H, the adjusted transient characteristics with  $H_t$  and the steady state characteristics.

Figure 7 shows that the difference between the transient and steady state characteristics in quadrant II and III are also removed by Nielsens method. Calculating  $Q_{ED}$  and  $n_{ED}$  from eq. (4) and eq. (5) for the transient characteristics use the measured H, the adjusted  $Q_{ED}$ - $n_{ED}$  characteristics use  $H_t$ . The transient characteristics with  $H_t$  and its correspondence to the steady state measurements and can thus be explained by the inertia of the water masses.

### 3.2 Uncertainty

Figure 8 show the repeatability for  $Q_{ED}$  vs  $n_{ED}$  for four repetitions at 10° guide vane opening.

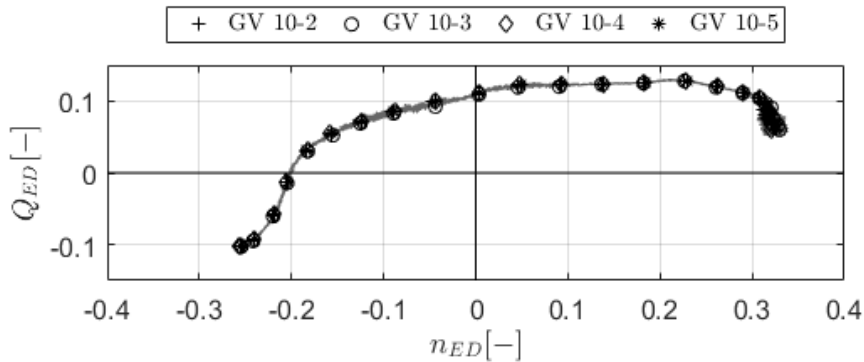


Fig. 8 The repeatability at 10° guide vane opening for measurement series 2 to 5

The absolute uncertainty for N and Q in the transient period  $T_D$  for one measurement series can be seen in Fig. 9. Where the uncertainty in the flow rate is shown in Fig. 9(b) and the uncertainty in the rotational speed is shown in Fig. 9(c). It is prudent to note that the uncertainty in flow measured during a transient phase makes it difficult to decide the standard deviation. In this experiment it was decided to use the standard deviation from  $T_{SS}$  when calculating the uncertainty in  $T_D$ . Due to the chosen standard deviation the uncertainty is probably marginally higher than calculated. For the rotational speed, it is noticeable that the uncertainty increases rapidly around zero. This is due to the encoders dependence on the pulses to determine the rpm. There are 1024 pulses for one rotation, but with close to zero rotation the result is a high increase in the uncertainty around that point. Excluding the uncertainty at zero, the mean absolute uncertainty,  $e_N$  for N is 0.0034 rpm. The mean absolute uncertainty,  $e_Q$  for the flow rate is 0.000156.

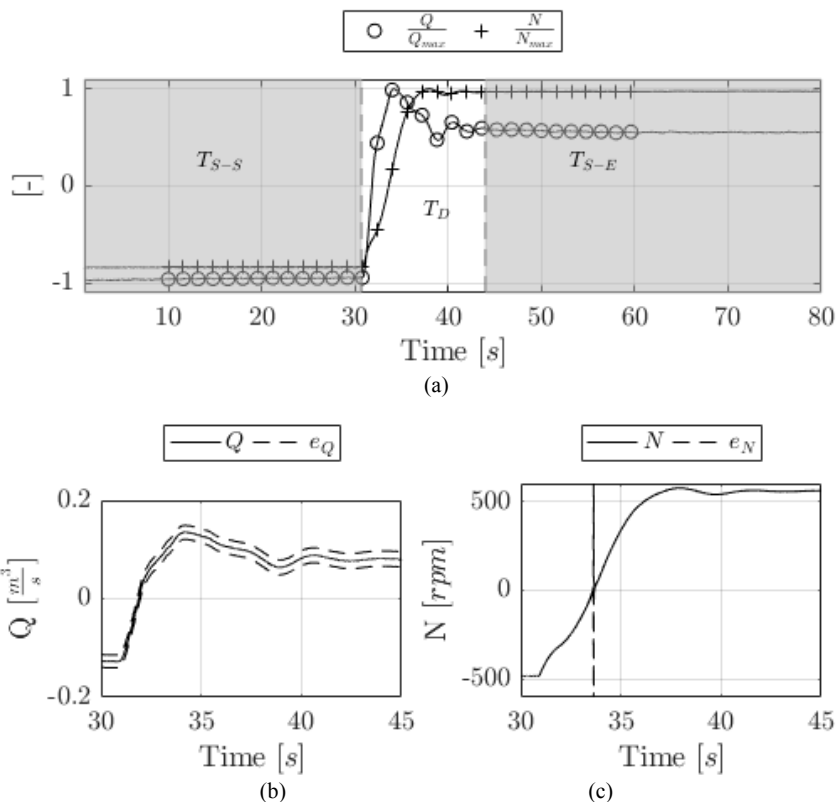


Fig. 9 (a) is the time dependent change in Q and N, (b) and (c) show the absolute uncertainty and the real value in the transient period TD for respectively Q and N. The uncertainty band is multiplied with 100 to enhance visibility

## 4. Discussion

The use of a modified pressure-time method for measuring the flow rate in a transient phenomena with big changes in the flow is previously unpublished. Nielsen [14] and Walseth [12] have used this method in the turbine mode of operation, but to the authors knowledge this is the first time the method is used to measure the transient flow from pump to turbine mode of operation. The uncertainty shown in Fig. 9(b) shows this method to be a reliable way to measure the flow.

There is a significant difference between the steady state and transient measurements in pump and pump break mode. Where, for the same flow, the rotational speed is smaller for the transient measurements than the steady state measurements. This phenomenon was also observed by Liu et al. [10] and Stens [9], but dismissed as an inaccuracy of the CFD in pump mode. The inertia of the water masses explains the difference. Nielsen [14] showed that by taking into account the inertia of the water masses removes the difference between the transient and steady state characteristics. The transient measurements are influenced by the system dynamics.

By accounting for this and subtracting the hydraulic inertia in the system from the head, we get the same results as in a steady state situation without system dynamics.

The pressure fluctuations that can be seen in Fig. 4(a) and Fig. 5 are highest where the discharge is low and at runaway speed in turbine mode of operation. This is in accordance with previous research by Zuo [1] and Tanaka [3], where it was found that these areas give the highest vibrations due to the off-design conditions.

In Fig. 4(b) the flow and rotational speed oscillations at runaway speed is reduced with lower opening degree on the guide vanes. These flow and speed oscillations are caused by the slower head oscillations seen in Fig. 5. The decrease in these oscillations dependent on the decrease in guide vane opening degree is because of the reduced flow through the turbine, and a smaller amplitude of the head oscillations after reaching the turbine quadrant (I). When doing a fast mode change ending at runaway speed it can therefore be recommended to do this in a manner that ends up at a low guide vane angle when the RPT reaches runaway speed. This can be done with a constant low GV angle from pump to turbine mode of operation, or with a gradual reduction in the GV angle during the transition.

## 5. Conclusion

This article presents an investigation of the transient characteristics of a reversible pump turbine, from pump to turbine mode of operation measured experimentally. It has been shown that the modified pressure time method is a reliable method to measure the discharge in this transient phase. Pressure fluctuations are highest where they can be expected to be, i.e at low discharge in both pump and turbine mode of operation and at runaway speed in turbine. The comparison of the steady state and transient characteristics show a difference in the pump mode due to the inertia of the water masses.

## Nomenclature

A	Area	[m]	Q	Flow rate	[m <sup>3</sup> /s]
B1	Inlet runner height	[m]	p	Pressure	[kPa]
D	Diameter	[m]	$\alpha$	Guide vane angle	[°]
g	Gravitational acceleration	[m/s <sup>2</sup> ]	$\beta$	Mean velocity component	[°]
GV	Guide vane angle	[°]	$\rho$	Density	[kg/m <sup>3</sup> ]
H	Head	[m]	$\zeta$	Friction loss	[-]
I	Hydraulic inertia	[1/s <sup>2</sup> ]	dt	Position indication	[-]
k	Friction factor	[-]	i1	Position indication	[-]
L	Length	[m]	o	Position indication	[-]
M	Torque	[Nm]	v1	Position indication	[-]
N,n	Rotational speed	[rad/s]	1	Inlet position turbine direction	[-]
nED	Non-dimensional speed	[-]	2	Outlet position turbine direction	[-]
QED	Non-dimensional flow	[-]	*	Best operation point	[-]

## References

- [1] Z. Zuo, S. Liu, Y. Sun, and Y. Wu, "Pressure fluctuations in the vaneless space of High-head pump-turbines—A review," *Renew. Sustain. Energy Rev.*, vol. 41, pp. 965–974, Jan. 2015.
- [2] E. Egusquiza, C. Valero, D. Valentin, A. Presas, and C. G. Rodriguez, "Condition monitoring of pump-turbines. New challenges," *Meas. J. Int. Meas. Confed.*, vol. 67, pp. 151–163, 2015.
- [3] H. Tanaka, "Vibration Behavior and Dynamic Stress of Runners of Very High Head Reversible Pump-turbines," *Int. J. Fluid Mach. Syst.*, vol. 4, no. 2, pp. 289–306, Jun. 2011.
- [4] L. Deyou, W. Hongjie, X. Gaoming, G. Ruzhi, W. Xianzhu, and L. Zhansheng, "Unsteady simulation and analysis for hump characteristics of a pump turbine model," *Renew. Energy*, vol. 77, pp. 32–42, May 2015.
- [5] G. Olimstad, T. Nielsen, and B. Borresen, "Stability limits of reversible-pump turbines in turbine mode of operation and measurements of unstable characteristics," *J. Fluids Eng.*, vol. 134, no. 11, p. 111202, Nov. 2012.
- [6] A. J. Stepanoff, *Centrifugal and axial flow pumps: theory, design, and application*, 2nd ed. New York: Wiley, 1957.
- [7] R. T. Knapp, "Complete characteristics of centrifugal pumps and their use in the prediction of transient behavior," *Trans. ASME*, pp. 683–689, 1937.
- [8] N. RUCHONNET and O. BRAUN, "Reduced scale model test of pump-turbine transition," in *IAHR WG Meeting on Cavitation*

and Dynamic Problems in Hydraulic Machinery and Systems.

[9] C. Stens and S. Riedelbauch, "Investigation of a fast transition from pump mode to generating mode in a model scale reversible pump turbine," IOP Conf. Ser. Earth Environ. Sci., vol. 49, p. 112001, Nov. 2016.

[10] J. Liu, S. Liu, Y. Sun, L. Jiao, Y. Wu, and L. Wang, "Three-dimensional flow simulation of transient power interruption process of a prototype pump-turbine at pump mode," J. Mech. Sci. Technol., vol. 27, no. 5, pp. 1305–1312, May 2013.

[11] G. Olimstad, "Design of a Reversible Pump-Turbine -with Purpose to Investigate Stability," presented at the 4th International Meeting on Cavitation and Dynamic Problems in Hydraulic Machinery and Systems, 2011.

[12] E. C. Walseth, T. K. Nielsen, and B. Svingen, "Measuring the Dynamic Characteristics of a Low Specific Speed Pump—Turbine Model," Energies, vol. 9, no. 3, p. 199, Mar. 2016.

[13] IEC, "Hydraulic turbines, storage pumps and pump-turbines - Model acceptance tests," Technical Standard NEK EN 60193:1999, 1999.

[14] Torbjørn K. Nielsen, "Transient characteristics of high head Francis turbines," Universitetet i Trondheim, Norges tekniske høgskole, Institutt for hydro- og gassdynamikk, Trondheim, 1990.

# Paper 2

**Pressure pulsations during a fast transition from pump to turbine mode of operation in laboratory and field experiment**

Svarstad, M. F., Nielsen, T. K.

*IOP Conference series* 2018



# Pressure pulsations during a fast transition from pump to turbine mode of operation in laboratory and field experiment

M F Svarstad and T K Nielsen

Waterpower laboratory, Department of Energy and Process Engineering, NTNU, Alfred Getz' vei 4, 7041 Trondheim, Norway

E-mail: [magni.f.svarstad@ntnu.no](mailto:magni.f.svarstad@ntnu.no)

**Abstract.** The reversible pump turbine (RPT) is a suitable machine to meet fluctuations in the energy market. The usage of RPTs for this purpose will increase the number of operational mode changes of the machine. In order to reduce the response time of the machine, fast transitions in the mode of operation are desired. Therefore, increased knowledge of how the machine operates during these fast transitions is needed. This paper presents measurements done both at the NTNU Waterpower Laboratory and Tevla Pump Power Plant. The two machines are not geometrically similar, and part of the result focus on the similarities in the measurements despite the differences in the two RPTs. Tevla is owned by the Norwegian company Nord-Trøndelag Energi (NTE) and consists of two reversible pump turbines. The installed capacity is 50 MW. The focus is on the pressure pulsations during the fast transition from pump to turbine mode of operation. Results from both the laboratory and field measurements show few but high pressure amplitudes during the fast transition.

## 1. Introduction

Balancing the fluctuations in the energy market, especially after the introduction of intermittent energy sources, are an important challenge. The reversible pump turbine (RPT) can be used to meet these fluctuations. To effectively use the RPT in this manner, the machine will experience an increase in the number of operational mode changes. In order to reduce the response time of the machine, fast transitions between the modes of operation are desired. How these fast transitions change the pressure pulsations experienced by the machine and penstock is important to know when evaluating a possible procedure change for the transition between pump and turbine mode of operation.

This article presents pressure measurements from the transient change from pump to turbine mode of operation. Results from both laboratory and full scale power plant test are shown and compared, even though the two cases are different not only in size, but also have different runner geometry, guide vane design and penstock. The focus is on the pressure pulsations during the fast transition from pump to turbine mode of operation.

The pressure pulsations in RPTs in off-design operation is a well researched area exemplified by Zuo et. al [1] in their review of pressure pulsations in vaneless space of a high head pump turbine. The most prominent pressure pulsations causing fatigue come from rotor stator interaction (RSI) and pressure pulsations that corresponds to the natural frequency (NF) of the

machine. In a transient operation the stochastic pressure pulsations (SPP) tend to be dominant [2]. With a highly transient phenomena like a fast mode change, there will be no time for the pressure pulsations that correspond to the natural frequency to develop any resonance. It is therefore most relevant to focus on the amplitudes themselves, rather than finding the natural frequency.

Braun and Ruchonnet [3] are among the few who have extended the research of pressure pulsations on to the area of operational mode transitions. In the laboratory experiments they did a number of transitions from pump to turbine mode of operation with different speeds. Their results indicate that the intensity of the pressure fluctuations in fact decreases with increased speed.

## 2. Method

The experiments presented in this article were conducted at the Waterpower Laboratory at NTNU and at Tevla pump power plant (Tevla). Tevla is a power plant with two reversible pump turbines (RPT) and an installed capacity of  $2 \cdot 25$  MW. Tevla is located in Nord-Trøndelag in Norway, and is owned by Nord-Trøndelag Energi (NTE).

The two turbines are not geometrically similar, as can be seen from their respective specific speeds ( $N_{QE}$ ) in Table 1 and Table 3. The results presented are thus not a comparison of a model with its prototype.

The area of investigation is the fast transition (FT) from pump to turbine mode of operation and the following pressure pulsations of this transition. The fast transition from pump to turbine start in normal pump mode of operation, where the wicket gate opening is reduced from optimal pump opening to a reduced opening. After the adjustment of the guide vanes, the connection between the generator/motor and the RPT is disconnected, in the same manner as in a load rejection scenario. Because of the pressure from the water masses the RPT will go from pump mode to runaway speed in turbine mode, and in the process traveling through pump break mode. At the same time, the wicket gate is kept open and constant in the reduced opening to avoid high runaway speed.

In the laboratory, it was not possible to reduce the wicket gate opening to the degree where the rotational speed corresponds to 50 Hz. The method was therefore carried out for a number of different guide vanes openings;  $4^\circ$ ,  $7^\circ$  and  $10^\circ$ . At Tevla, the reduced wicket gate opening corresponds to  $\alpha_{idle}$ , the opening that gives nominal speed at runaway in turbine mode of operation, i.e the opening degree for turbine start up. The RPT therefore ends up at the ideal position to reconnect the generator and connect the machine to the grid. The method was first tested in the laboratory, and later carried out at Tevla. The only difference was the reduced wicket gate opening.

### 2.1. Laboratory tests

When doing transient experiments it is important to remove disturbances on the system caused by the pump supplying the head. The Francis test rig was therefore arranged to operate in an open loop configuration. In order to disconnect the hydraulic inertia of the outlet system a weir was installed in the outlet tank. The laboratory set-up was the same as used by Eve Walseth [4]. Figure 1 show the sensor placements in the test rig and Table 2 show the instrument parameters, and have a sampling rate of 5000 Hz.

The model runner is designed by Grunde Olimstad [5] during his PhD work. The runner parameters from a turbine perspective are listed in Table 1, and in accordance with IEC 60193 [6, p. 26] 1 is the high pressure side, and 2 is the low pressure side.

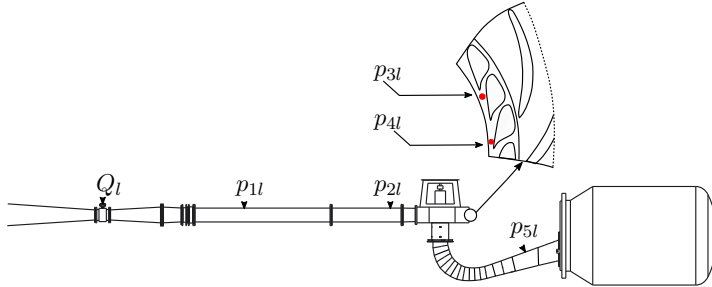


**Figure 1.** Sensor placement laboratory measurements.

**Table 1.** RPT - turbine properties.

$D_1$	$D_2$	$B_1$	$n_{ED}^*$	$Q_{ED}^*$	$H^*$	$\beta_1$	$\beta_2$	$\alpha^*$	$N_{QE}$
0.631 m	0.349 m	0.059 m	0.133	0.223	29.3 m	12°	12.8°	10°	0.0628

**Table 2.** Laboratory sensor parameters.

Sensor	Type	Range	Precision
$p_{2l}$	UNIK 5000	10 bar	0.1 %
$p_{3l}$	Kulite XTE190	7 bar	0.5 %
$p_{4l}$	Kulite XTE190	7 bar	0.5 %
$p_{5l}$	UNIK 5000	5 bar	0.1 %

## 2.2. Tevla tests

One of the turbines was used in the test presented. During the experiment the other turbine was at standstill with the main inlet valve closed. The execution of the fast transition required an operation of the power plant outside of normal procedures. A number of protection systems were shut of so as not to trigger the normal shutdown procedure if the power plant experience a load rejection. Then the control system was turned to manual and the wicket gates were manually adjusted to to  $\alpha_{idle}$ . Finally the main circuit breaker was turned, disconnecting the generator from the grid and leading to the fast transition. Due to the complexity of a modern power plant, a number of attempts were needed to find the correct method to bypass the fail-safes in the system. The end result was therefor one successful completion of the fast transition.

**Table 3.** Tevla parameters.

$P$	$\alpha^*$	$\alpha_{idle}$	$H_{net}$	$N_{QE}$
25 MW	53.9 %	14.7 %	148.4 m	0.126

The sensor placement at Tevla was decided by existing pressure taps. The difference from the laboratory setup were the lack of pressure measurements in the vaneless space. Instead two

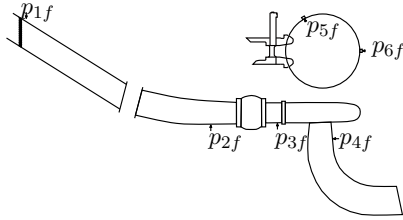


**Figure 2.** Sensor placement field measurements.

**Table 4.** Tevla instrument parameters.

Sensor	Type	Range	Precision
$p_{3f}$	UNIK 5000	50 bar	0.1 %
$p_{4f}$	UNIK 5000	10 bar	0.1 %
$p_{5f}$	UNIK 5000	50 bar	0.1 %
$p_{6f}$	UNIK 5000	100 bar	0.1 %

pressure taps at the spiral casing was accessible. The position of the pressure sensors are shown in Figure 2 and the instrument parameters can be seen in Table 4.

### 2.3. Data processing

The Rainflow counting method is commonly used for cycle counting in fatigue analysis [2]. The principle can be used just as well to analyze pressure amplitudes. When doing transient measurements where the pressure pulsations are stochastic, the use of Fast Fourier Transform (FFT) is inconvenient, since the pulsations doesn't occur at certain frequencies. Using the pressure measurements together with the sample rate of 5000 Hz with the Rainflow method gives the amplitude of the pressure pulsations together with the number of cycles each amplitude occurs. The Rainflow method is described in the standard *ISO 12110* [7].

When analyzing the pressure pulsations from both the laboratory and the field measurements, the lowest amplitudes have been disregarded. The area of interest are on the pressure amplitudes outside the ranges found during normal operation. In both cases, pressure pulsations measured at Best Efficiency Point (BEP) in turbine mode of operation have been used as the basis for this low amplitude threshold.

## 3. Results and Discussion

The fast transition start at steady state pump operation, marked in Figure 3 by  $A'$ . When the generator is disconnected the RPT gradually decreases in flow rate and rotational speed through quadrant  $A$ . The flow rate changes direction first, and the RPT enters quadrant  $B$ , the pump break mode. In quadrant  $B$  the rotational speed is still in the pump direction, but the flow is now going downstream, as in turbine mode of operation. When the rotational speed reaches zero and starts to accelerate the RPT is in quadrant  $C$ , turbine mode of operation. The next steady state condition is the runaway speed in turbine mode of operation. The measured pressure pulsations are shown in the subsections for the laboratory and field measurements respectively. Figure 4 and Figure 6 show the rated amplitude of each pressure pulsation with respect to time for laboratory and field measurements respectively. The figures also have numbering explaining

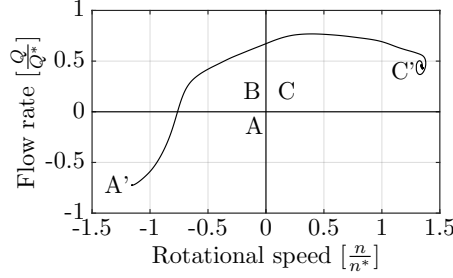


**Figure 3.** Illustration of  $N - Q$  characteristic of the fast transition.

where in the characteristics plot the different amplitudes occur. The rated amplitude  $A_R$  [%], is defined in Equation 1.

$$A_R = \frac{Amp}{H_{net}} \cdot 100 \quad (1)$$

Where  $Amp$  is the amplitude of the pressure pulsations and  $H_{net}$  is the head at optimal turbine operation. From the Rainflow method the minimum and maximum amplitudes for each pressure sensor have been found. All the amplitudes have been divided into ten sections presented by its average as the x-axis in Figure 5 and Figure 7 for laboratory and field tests respectively. The ten amplitude sections have a range  $\Delta R$  from displayed average value by  $\pm 5\%$  of the maximum amplitude.

### 3.1. Laboratory measurements

In the laboratory experiment the transition took approximately 8 s and is similar for the different wicket gate openings. As can be seen in Figure 4, the trend in the pressure amplitudes are also the same. The highest amplitudes are found in pump break mode (Section 3) and in the beginning of turbine mode of operation. In Figure 4, section 1 is the period before the fast transition, i.e. the steady state pump operation. In section 2, ranging from the start of transient period to the beginning of pump break mode, the increase in amplitudes are first seen at the end of the section. Section 4 is in turbine mode of operation from  $n_{ED} = 0$  to when  $Q_{ED}$  reaches maximum value. Section 5 is from  $Q_{ED}$  maximum to  $n_{ED}$  maximum. Section 6 is runaway speed. The amplitude magnitude have the same trend with respect to time for all the pressure sensors, even though the ranges differ. The highest amplitudes can be seen in the vaneless space by sensor  $p_{3l}$  and  $p_{4l}$ . The lowest amplitude is found by the outlet sensor  $p_{5l}$ .

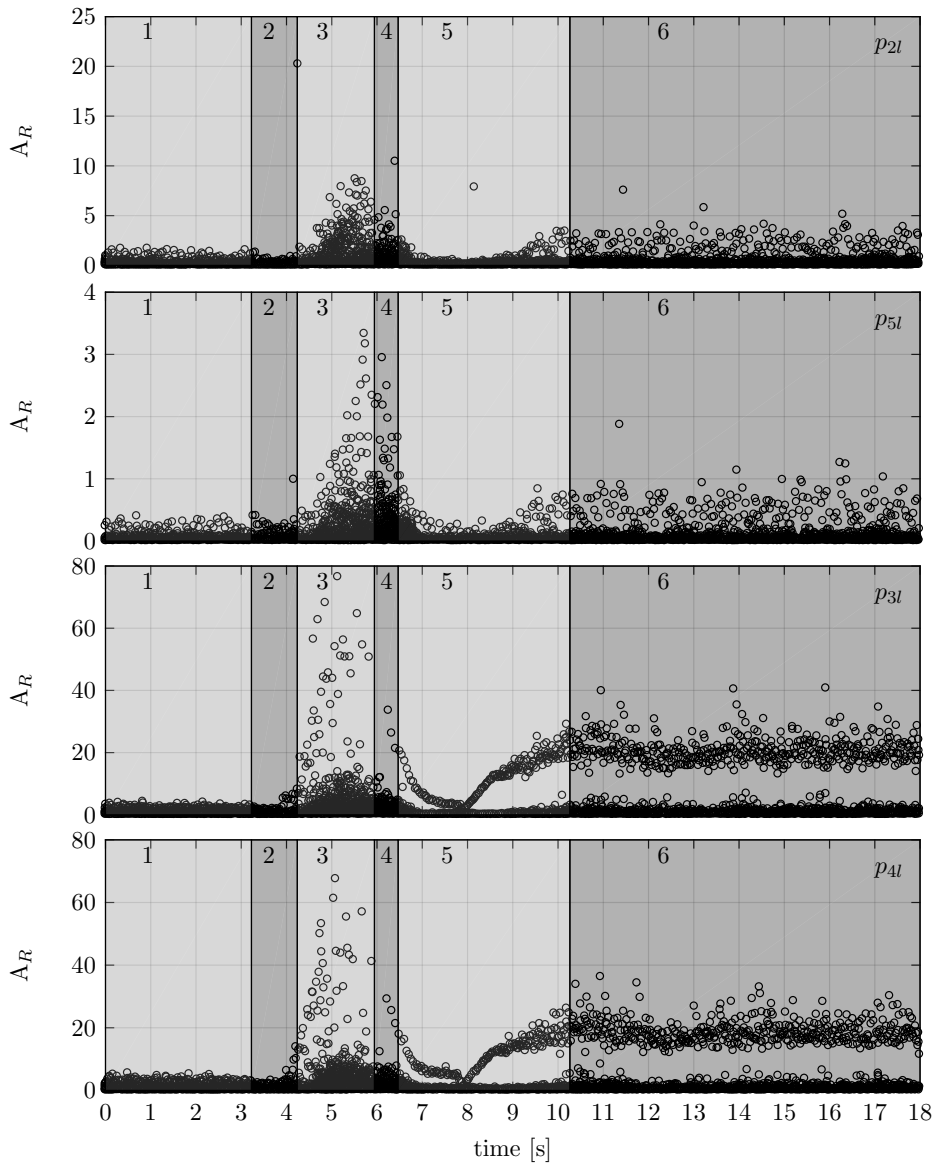


**Figure 4.** The rated amplitude ( $A_R$ ) for pressure sensors during the fast transition in laboratory. The position of  $p_{2l}$ ,  $p_{5l}$ ,  $p_{3l}$  and  $p_{4l}$  can be seen in Figure 1.

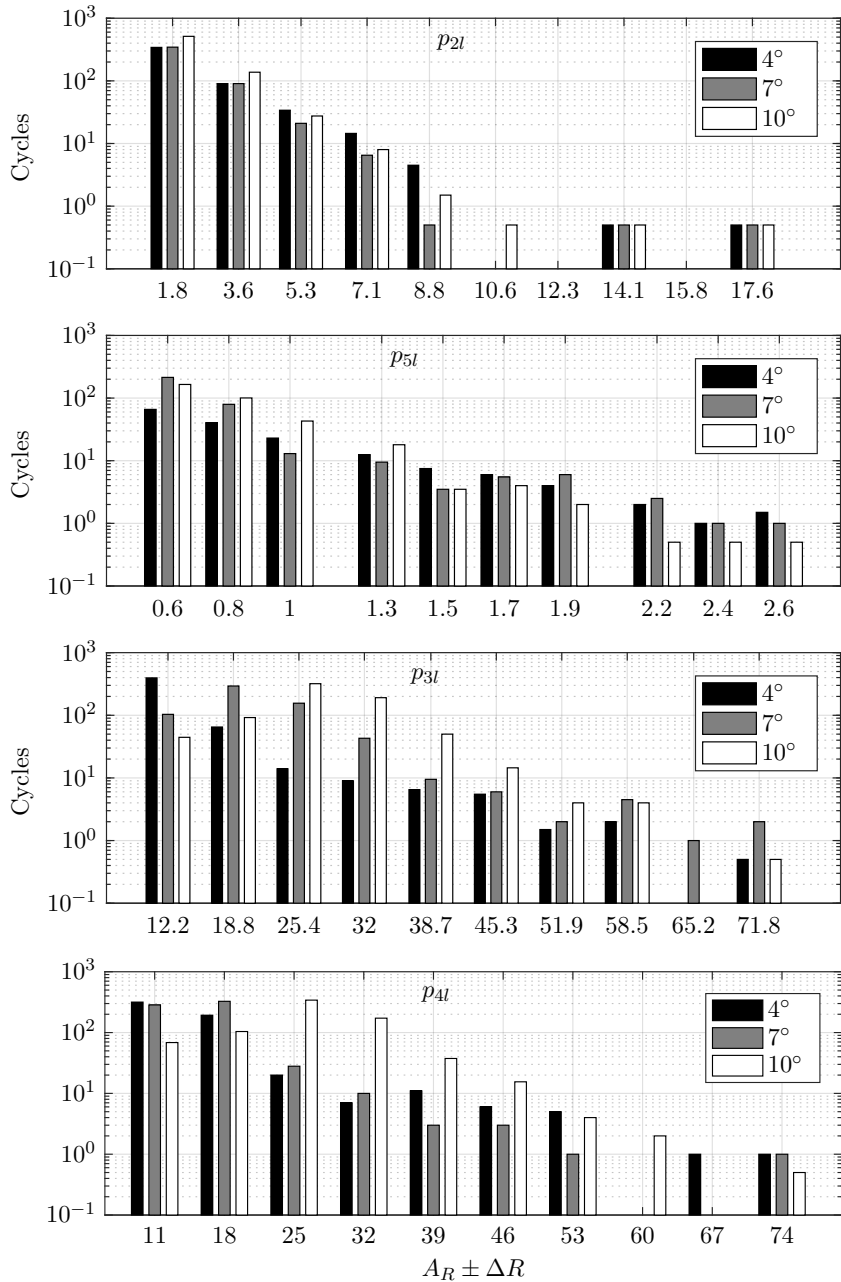


**Figure 5.** The number of cycles for all amplitudes ( $A_R$ ) during the fast transition in laboratory.  $\Delta R$  is 0.93, 0.53, 1.38 and 1.47 respectively for  $p_{2l}$ ,  $p_{5l}$ ,  $p_{3l}$  and  $p_{4l}$ .

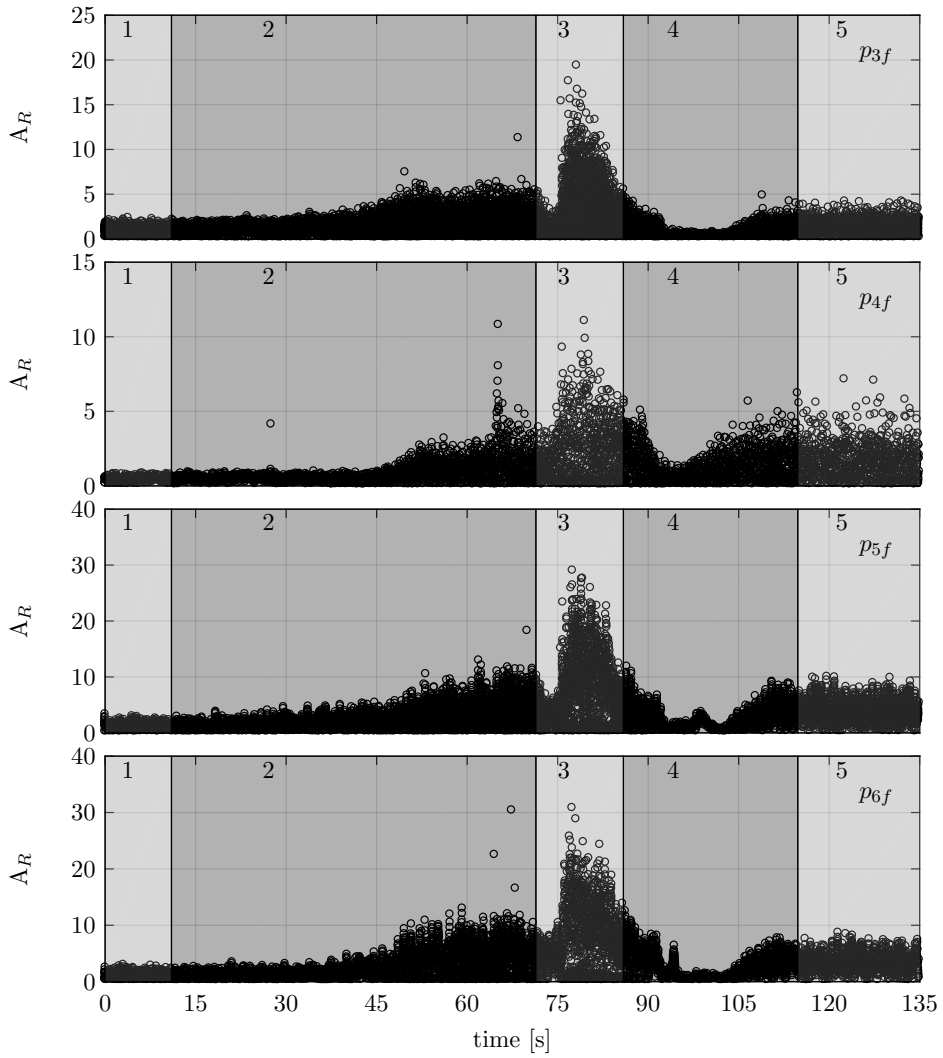


**Figure 6.** The rated amplitude ( $A_R$ ) for pressure sensors during the fast transition at Tevla. The position of  $p_{3f}$ ,  $p_{4f}$ ,  $p_{5f}$  and  $p_{6f}$  can be seen in Figure 2.

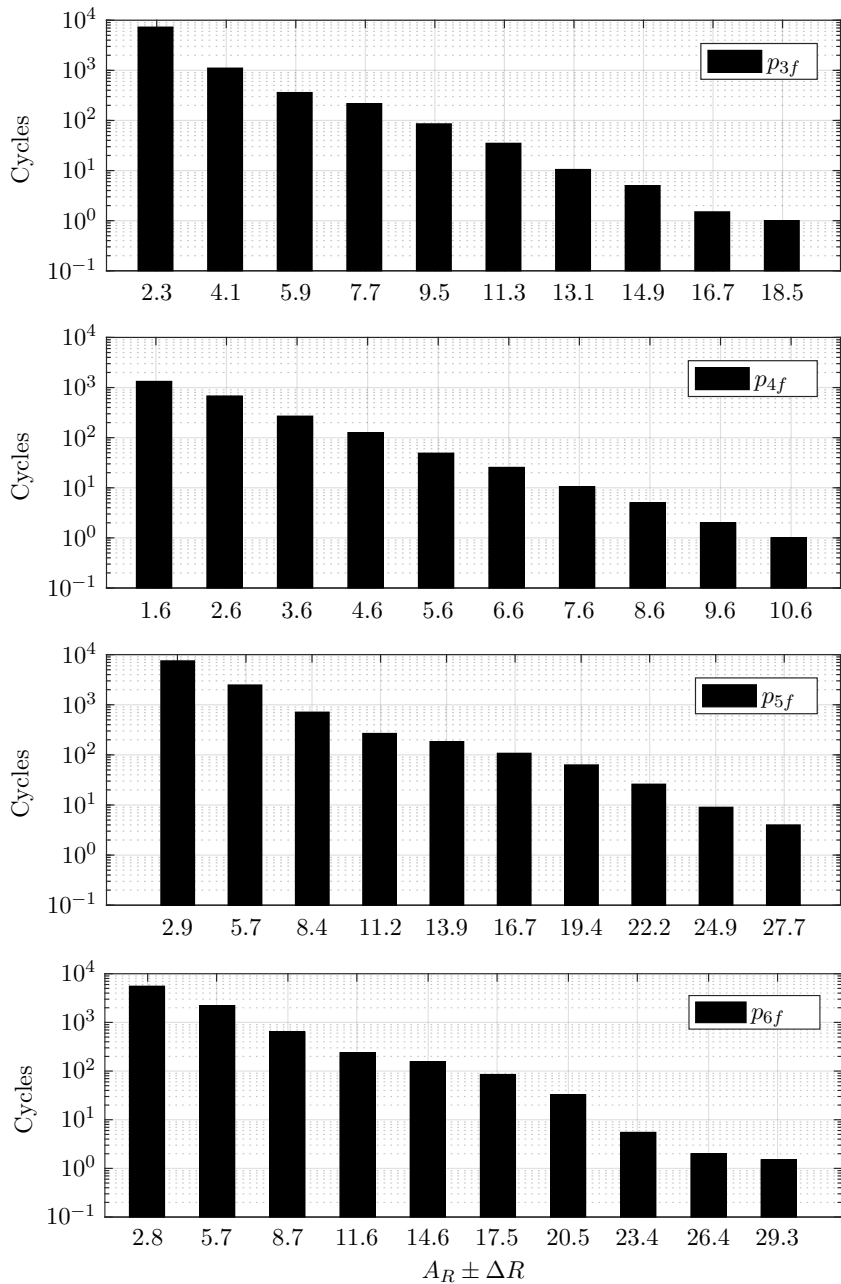


**Figure 7.** The number of cycles for all amplitudes ( $A_R$ ) during the fast transition at TevL.  $\Delta R$  is 0.92, 0.52, 1.38 and 1.46 respectively for  $p_{3f}$ ,  $p_{4f}$ ,  $p_{5f}$  and  $p_{6f}$ .

Figure 5 show the summation of all the pressure amplitude cycles for the three different wicket gate openings. All of the results show a high number of small amplitudes. The number of cycles decreases with increasing mean amplitude. The highest wicket gate opening of  $10^\circ$  have the smallest number of high amplitudes for all pressure sensors. In the mid range area the increase in wicket gate opening results in a higher number cycles in the vaneless space.

### 3.2. Field measurements

The field measurements start at optimal wicket gate opening in pump mode of operation and are first reduced to  $\alpha_{idle}$ , marked by the start of section 2 in Figure 6. The beginning of section 3 marks the start of the fast transition. Section 3 includes both pump and pump break mode of operation and the maximum amplitudes are in this area. The start of section 4 also have high amplitudes. Section 4 is the turbine mode of operation from  $n_{ED} = 0$  to when  $n_{ED}$  reaches maximum value. Section 5 is runaway speed. The fast transition at Tevla took 43 s. The sensors closest to the runner show the highest amplitudes. The maximum amplitudes in Figure 7 are few, including the top two columns none exceeds ten cycles.

### 3.3. Comparison

For both the laboratory and field experiment the results show similar trends. In both cases the hydraulic pressure is the driving force for the fast transition, the subsequent rotational speed and velocity components of the flow causes the pressure pulsations. For all RPTs, even with different specific speed, the operating points with unfavorable flow conditions will cause the higher pressure pulsations. The pressure amplitudes are highest in pump break mode but consists of few number of cycles. Most pressure sensors have one cycle at the highest pressure amplitude and none of the pressure sensor have more than four cycles for the highest amplitudes. The highest relative amplitudes in the laboratory experiment are as high as 71.8%. For the measurements at Tevla the highest relative amplitudes are 29.3%. Since the pressure is measured at two different places with respect to the turbine runner this does not mean that the fast transition at Tevla necessarily experience lower relative pressure amplitudes.

## 4. Conclusion

The fast transition from pump to turbine mode of operation was successfully conducted both in the laboratory and at Tevla. The laboratory test rig and power plant are different not only in size, but also have different runner geometry, guide vane design and penstock. With all of these differences, the comparison between the two experiments nevertheless show clear similarities. The highest pressure amplitudes occur in the pump break mode. The high amplitudes experienced in this area is the most relevant objection against this method of changing from pump to turbine mode of operation. The pump break mode is an area not entered during a normal start and stop, neither in pump or turbine mode of operation.

### Acknowledgments

The authors would like to thank Nord-Trøndelag Energi (NTE) for giving us access to Tevla pump power plant, and all the help given during the planning and execution of the experiment. We would also like to thank Hymatek AS for lending us their expertise on turbine regulators in the planning and during the tests.

## References

- [1] Zuo Z, Liu S, Sun Y and Wu Y 2015 *Renewable and Sustainable Energy Reviews* **41** 965–974  
ISSN 1364-0321

- [2] Huang X, Chamberland-Lauzon J, Oram C, Klopfer A and Ruchonnet N 2014 *IOP Conference Series: Earth and Environmental Science* **22** 012014 ISSN 1755-1315
- [3] Braun O and Ruchonnet N 2017 *J. Phys.: Conf. Ser.* vol 813 p 012017
- [4] Walseth E C, Nielsen T K and Svingen B 2016 *Energies* **9** 199
- [5] Olimstad G 2011 *Proc. of the 4th International Meeting on Cavitation and Dynamic Problems in Hydraulic Machinery and Systems (Belgrade, Serbia)*
- [6] IEC 1999 Hydraulic turbines, storage pumps and pump-turbines - Model acceptance tests Technical Standard IEC 60193:1999
- [7] ISO 12110-2:2013 - Part 2: Cycle counting and related data reduction methods



# Paper 3

**A comparison of pressure pulsations during normal and fast transition from pump to turbine mode of operation**

Svarstad, M. F., Nielsen, T. K.

*Submitted 2018*

This paper is awaiting publication and is not included in NTNU Open



# Paper 4

**Four quadrant characteristics simulated with 1D RPT model**

Svarstad, M. F., Nielsen, T. K., Storli P. T.

*Submitted 2018*

This paper is awaiting publication and is not included in NTNU Open